Electronic Supplementary Material (ESI) for Chemical Communications.

Supporting Information

Transition between tangential and co-axial liquid crystalline honeycombs in the self-assembly of Y-shaped bolapolyphiles

Anne Lehmann[1], Marko Prehm[1], Changlong Chen[2], Feng Liu[2,*], Xiangbing Zeng[3], Goran Ungar[3*], Carsten Tschierske[1,*]

[1] Department of Chemistry, Martin Luther University Halle-Wittenberg, Kurt-Mothes-Str. 2, 06120 Halle, Germany

[2] State Key Laboratory for Mechanical Behavior of Materials, Xi'an Jiaotong University, Xi'an 710049, P. R. China

[3] Department of Materials Science and Engineering, Sheffield University, Sheffield S1 3JD, UK

1. Experimental techniques

1.1 XRD

X-ray scattering on aligned samples. - X-ray investigations were carried out at Cu Kα line (λ = 1.54 Å) using a standard Coolidge tube source with a Ni-filter. Aligned samples were obtained on a glass plate on a temperature-controlled heating stage. Alignment was achieved upon slow cooling (rate: 1 K·min^{-1} – 0.01 K·min^{-1}) of a small droplet of the sample and takes place at the sample–glass or at the sample–air interface. The aligned samples were held on a temperature-controlled heating stage and the diffraction patterns were recorded with a 2D detector (HI-STAR, Siemens); the exposure time was 15 min for WAXS and 30 min for SAXS. The distance between the sample and the detector was 9.0 cm (WAXS) or 26.8 cm (SAXS), and the beam was parallel to the substrate.

Synchrotron X-ray diffraction and electron density reconstruction.− High-resolution small-angle powder diffraction experiments were recorded on Beamline I22 at Diamond Light Source and Beamline BL16B1 at Shanghai Synchrotron Radiation Facility, SSRF. Samples were held in evacuated 1 mm capillaries. A modified Linkam hot stage with a thermal stability within 0.2 ºC was used, with a hole for the capillary drilled through the silver heating block and mica windows attached to it on each side. A MarCCD detector was used. q calibration and linearization were verified using several orders of layer reflections from silver behemate and a series of n-alkanes. The measurement of the positions and intensities of the diffraction peaks is carried out using Galactic PeakSolve^{TM} program, where experimental diffractograms are fitted using Gaussian shaped peaks. The diffraction peaks are indexed on the basis of their peak positions, and the lattice parameters and the space groups are subsequently determined. Once the diffraction intensities are measured and the corresponding space group determined, 3-d electron density maps can be reconstructed, on the basis of the general formula

$$E(xyz) = \Sigma_{hkl}\, F(hkl) \exp[\mathrm{i}2\pi(hx+ky+lz)] \qquad \text{(Eqn. 1)}$$

Here $F(hkl)$ is the structure factor of a diffraction peak with index (hkl). It is normally a complex number and the experimentally observed diffraction intensity

$$I(hkl) = \mathrm{K}\cdot F(hkl)\cdot F^{*}(hkl) = \mathrm{K}\cdot |F(hkl)|^2 \qquad \text{(Eqn. 2)}$$

Here K is a constant related to the sample volume, incident beam intensity etc. In this paper we are only interested in the relative electron densities, hence this constant is simply taken to be 1. Thus the electron density

$$E(xyz) = \Sigma_{hkl}\, \mathrm{sqrt}[I(hkl)] \exp[\mathrm{i}2\pi(hx+ky+lz)+\phi_{hkl}] \qquad \text{(Eqn. 3)}$$

for 2D structures $I(hk)$ and Eqn. (4) were used:

$$E(xy) = \Sigma_{hk}\, \mathrm{sqrt}[I(hk)] \exp[i2\pi(hx+ky) +\phi_{hk}] \qquad \text{(Eqn. 4)}$$

As the observed diffraction intensity $I(hk)$ is only related to the amplitude of the structure factor $|F(hk)|$, the information about the phase of $F(hk)$, ϕ_{hk}, can not be determined directly from experiment. However, the problem is much simplified when the structure of the ordered phase is centrosymmetric, and hence the structure factor $F(hk)$ is always real and ϕ_{hk} is either 0 or π.

This makes it possible for a trial-and-error approach, where candidate electron density maps are reconstructed for all possible phase combinations, and the "correct" phase combination is then selected on the merit of the maps, helped by prior physical and chemical knowledge of

the system. This is especially useful for the study of nanostructures, where normally only a limited number of diffraction peaks are observed.

GISAXS experiments were carried out on station BM28 (XMaS line) at ESRF. Thin films were prepared from the melt on a silicon wafer. The thin film coated 5 x 5 mm^2 Si plates were placed on top of a custom built heater, which was then mounted on a six-circle goniometer. A MarCCD 165 detector at ESRF was used. The sample enclosure and the beam pipe were flushed with helium.

1.2 POM and DSC

Polarizing Optical Microscopy (POM). Transition temperatures were measured using a Mettler FP-82 HT hot stage and control unit in conjunction with a Leica DMRXP polarizing microscope (Leica Microsystems GmbH, Wetzlar, Germany). Textures of the liquid crystalline mesophases were recorded with a Leica MC120 HD camera (Leica Microsystems GmbH, Wetzlar, Germany).

DSC measurements. DSC-thermograms were recorded on a DSC-7 (Perkin-Elmer GmbH & Co. KG, Überlingen, Germany) in 30 μL Al-pans with heating and cooling rates of 10 K_min-1.

1.3 MD simulation

Annealing dynamics runs were carried out using the Universal Force Field (Material Studio, Accelrys). The structures in Fig. S20 were obtained with either 4 molecules in a square prism box or 20 molecules in a rectangular prism box and a height of 0.45nm, with 3d periodic boundary conditions. 30 temperature cycles of NVT dynamics were run between 300 and 700 K, with a total annealing time of 30 ps.

2. Additional Data

2.1 DSCs and phase transitions

Table S1. Phase transition temperatures (DSC peak temperatures, 10 K min^{-1}) and corresponding transition enthalpy values [ΔH (kJ mol^{-1})] of compounds **A*n*** on heating (H) and cooling (C) [a]

A*n*	Phase transitions
A5	H: Cr 167 [18.5] SmA+ 206 [6.2] Iso C: Iso 203 [6.7] SmA+ 114 [18.2] Cr
A7	H: Cr 156 [22.8] SmA+ 194 [6.4] Iso C: Iso 191 [6.6] SmA+ 105 [16.2] Cr
A8	H: Cr 156 [24.7] SmA+ 190 [5.8] Iso C: Iso 187 [6.0] SmA+ 116 [0.8] *P*6/*mmm* 101 [18.1] Cr
A9	H: Cr 145 [20.7] SmA+ 186 [4.9] Iso C: Iso 182 [5.2] SmA+ 130 [0.8] *P*6/*mmm* 95 [-] M 65 [2.4][b] Cr
A10	H: Cr 150 [26.8] (Col_{squ}/*p*4*mm* 124 [1.8]) *P*6/*mmm* 159 [0.9] SmA+ 184 [4.5] Iso C: Iso 182 [4.7] SmA+ 157 [1.0] *P*6/*mmm* 115 [1.8] Col_{squ}/*p*4*mm* 78 [11.3] Cr
A11	H: Cr 151 [24.0] (Col_{squ}/*p*4*mm* 140 [2.6]) *P*6/*mmm* 168 [1.0] SmA+ 181 [4.0] Iso C: Iso 179 [4.0] SmA+ 164 [1.2] *P*6/*mmm* 136 [2.4] Col_{squ}/*p*4*mm* 84 [13.4] Cr
A12	H: Cr 152 [26.8] (Col_{squ}/*p*4*mm* 137 [2.0]) *P*6/*mmm* 170 [1.4] SmA+ 179 [3.5] Iso C: Iso 178 [3.5] SmA+ 169 [1.4] *P*6/*mmm* 131 [2.3] Col_{squ}/*p*4*mm* 98 [17.1] Cr
A13	H: Cr 158 [27.5] (Col_{squ}/*p*4*mm* 140 [2.8]) *P*6/*mmm* 174 [1.6] SmA+ 177 [2.9] Iso C: Iso 177 [3.0] SmA+ 172 [1.7] *P*6/*mmm* 141 [3.2] Col_{squ}/*p*4*mm* 107 [18.4] Cr
A14	H: Cr 159 [29.7] Col_{rec}/*p*2*gg* 182 [6.5] Iso C: Iso 179 [6.2] Col_{rec}/*p*2*gg* 129 [26.0] Cr

[a] H = heating, C = cooling; additional values in brackets were taken from the second heating scan; M = unknown mesophase; [b] only partial crystallisation.

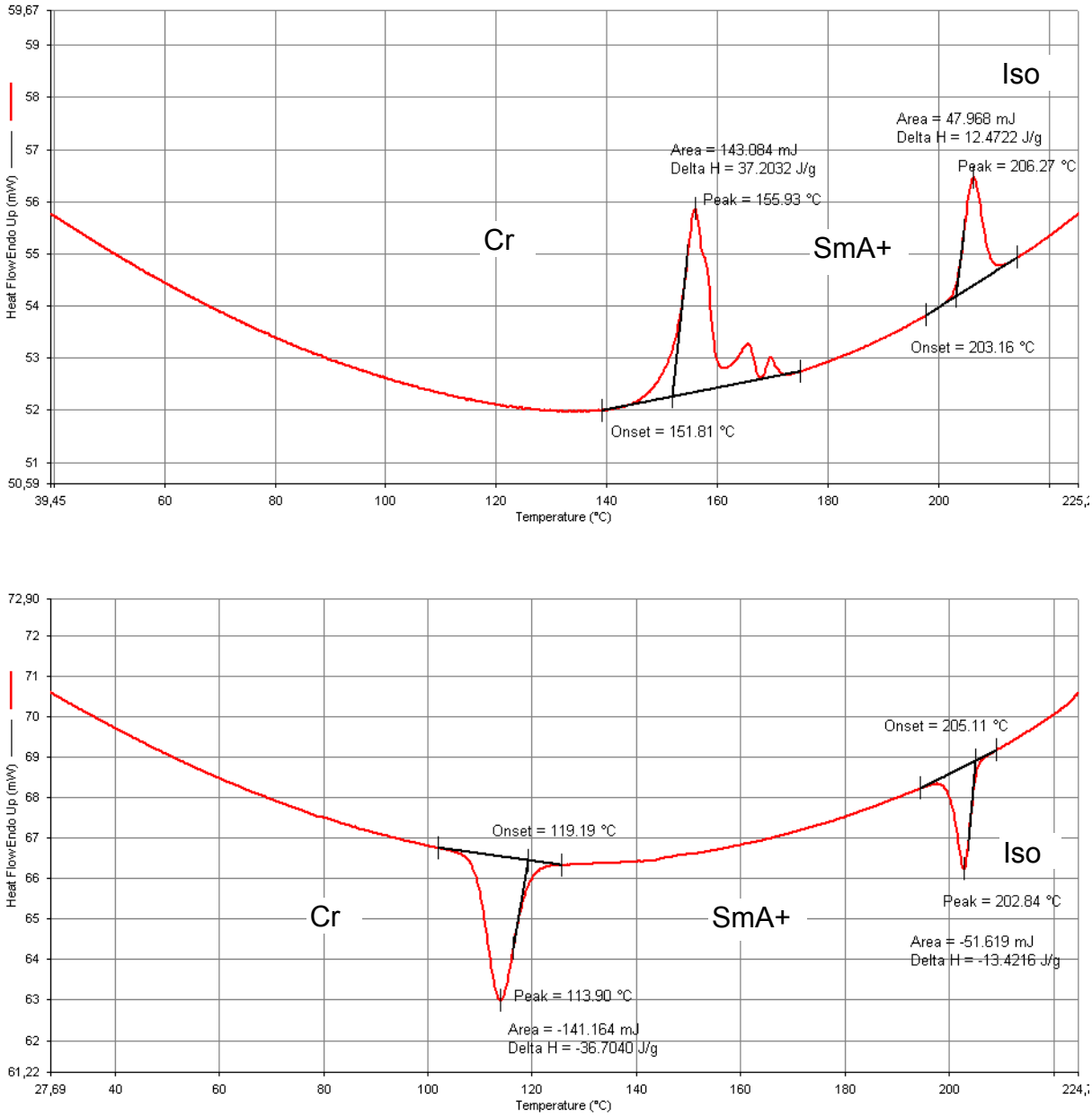

Figure S1a. Second DSC heating (top) and cooling scans (bottom) of compound **A5** at 10 K min^{-1}.

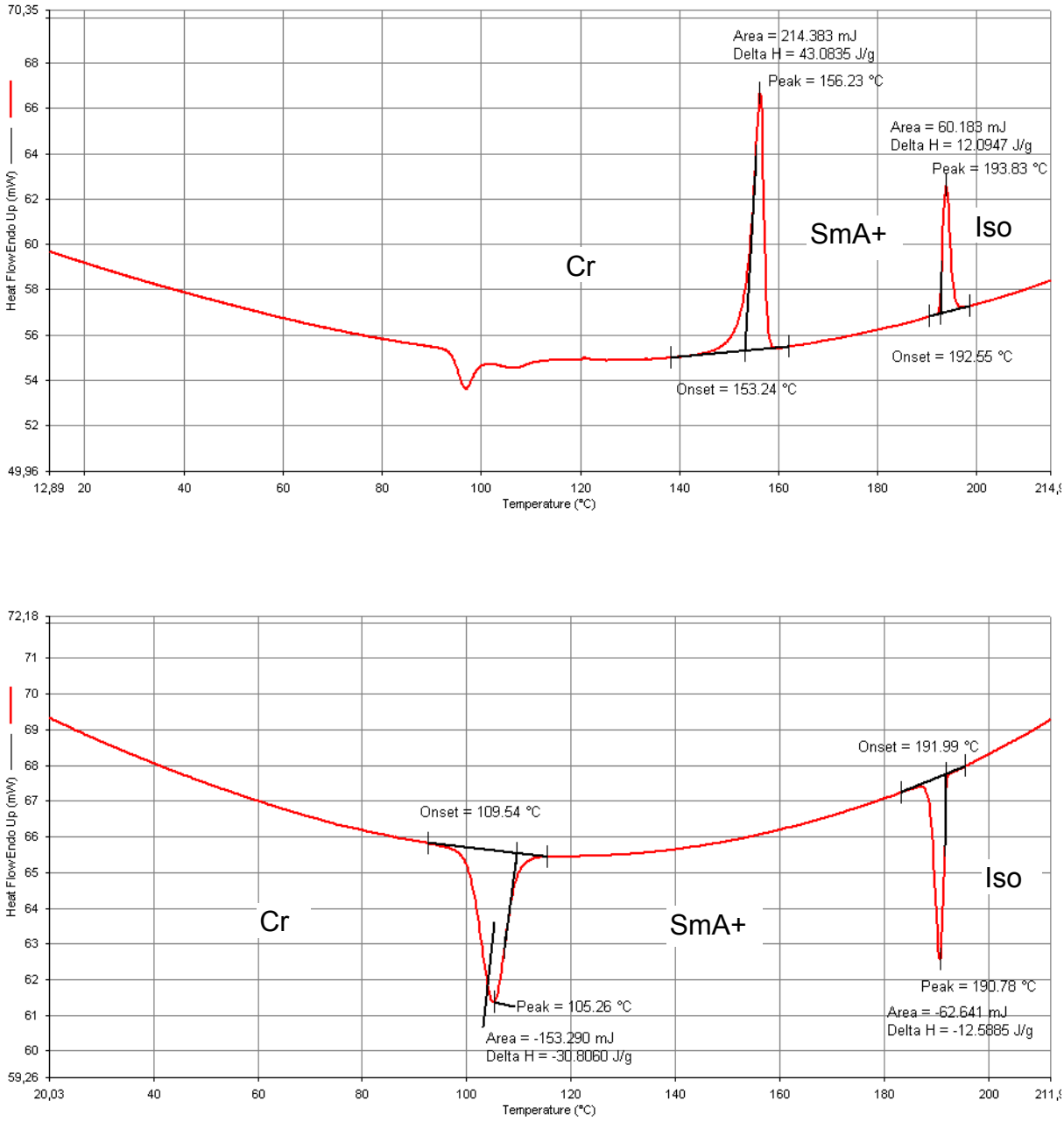

Figure S1b. First DSC heating (top) and cooling scans (bottom) of compound **A7** at 10 K min^{-1}.

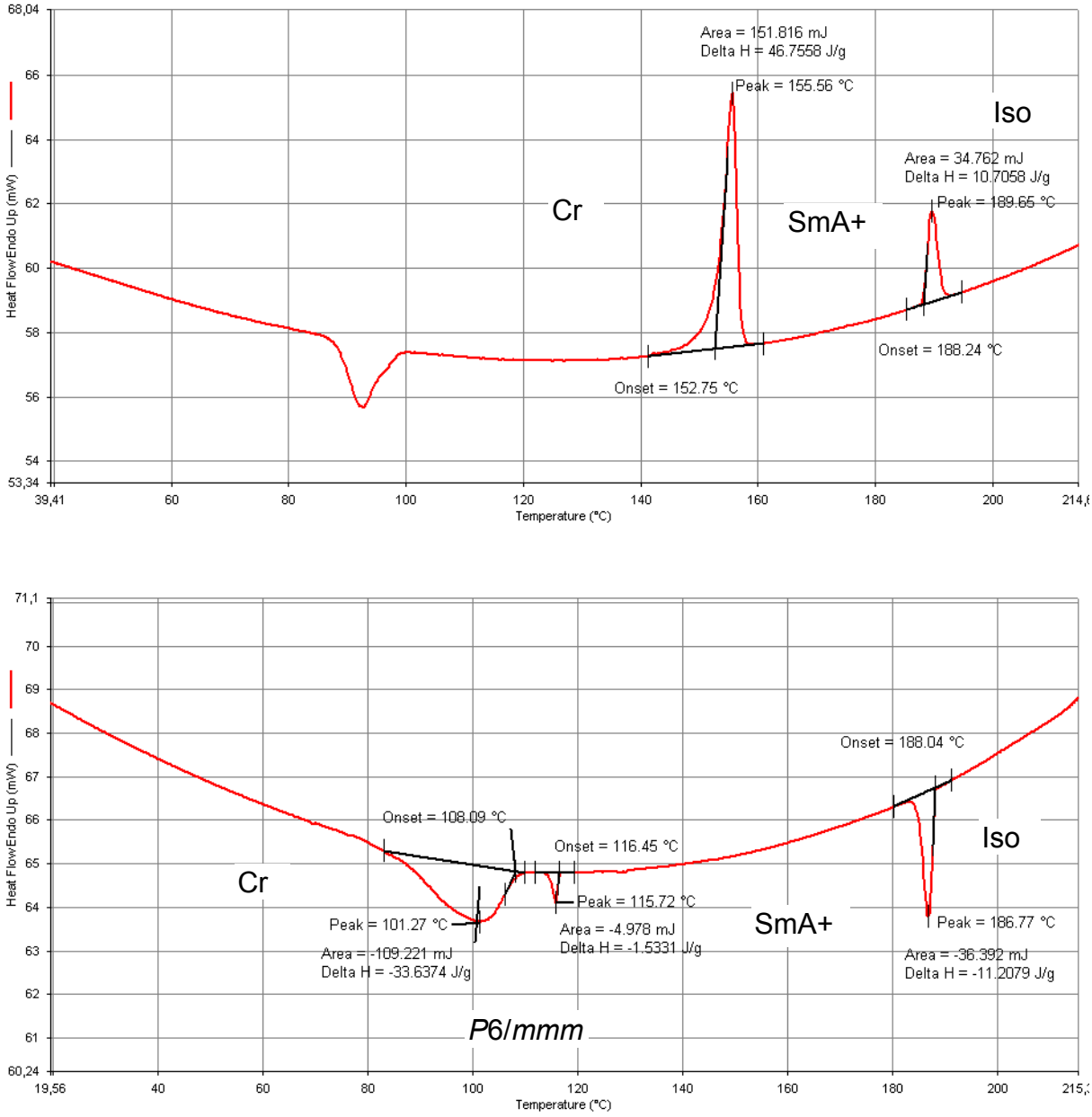

Figure S1c. First DSC heating (top) and cooling scans (bottom) of compound **A8** at 10 K min^{-1}.

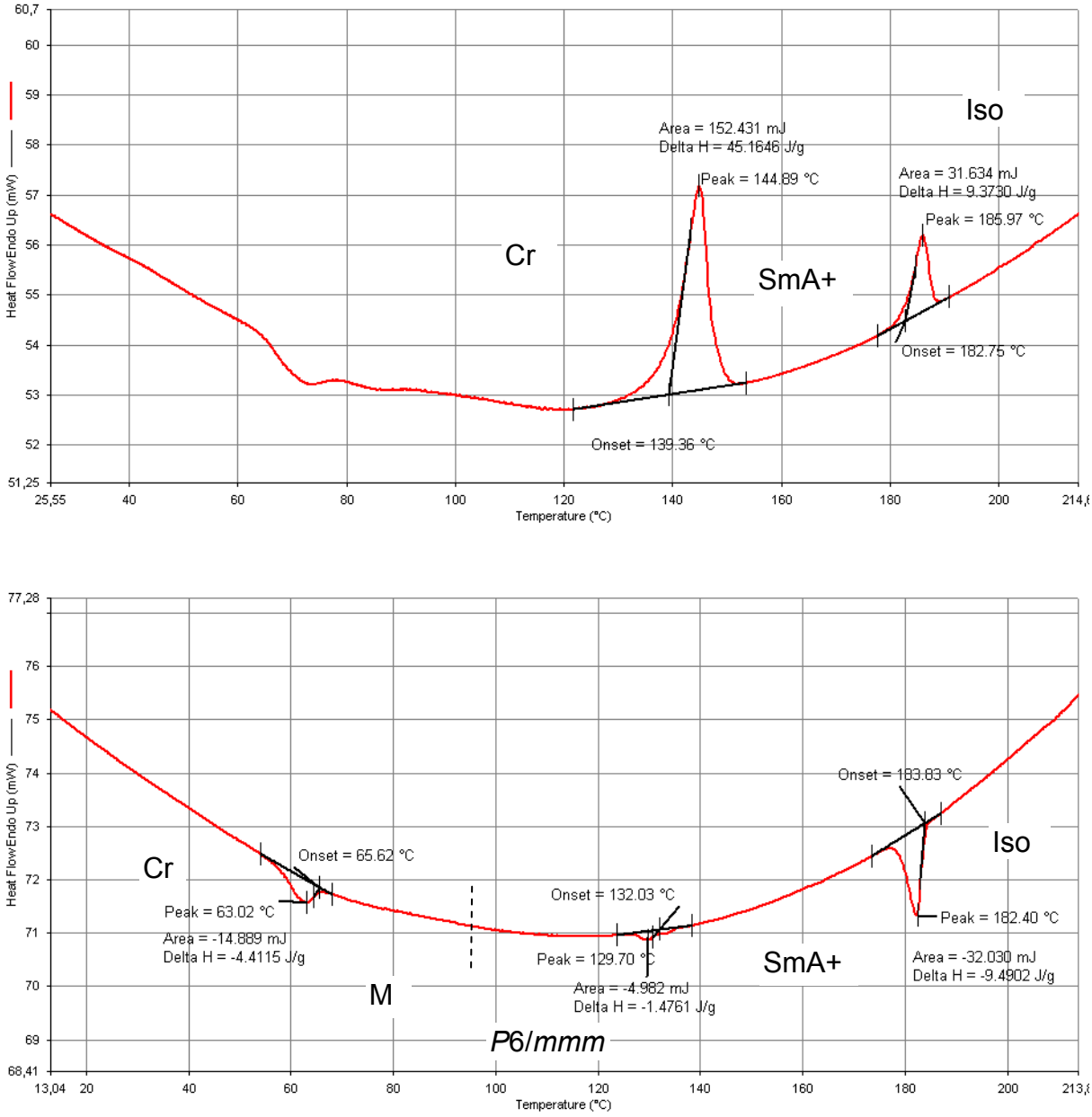

Figure S1d. First DSC heating (top) and cooling scans (bottom) of compound **A9** at 10 K min^{-1}.

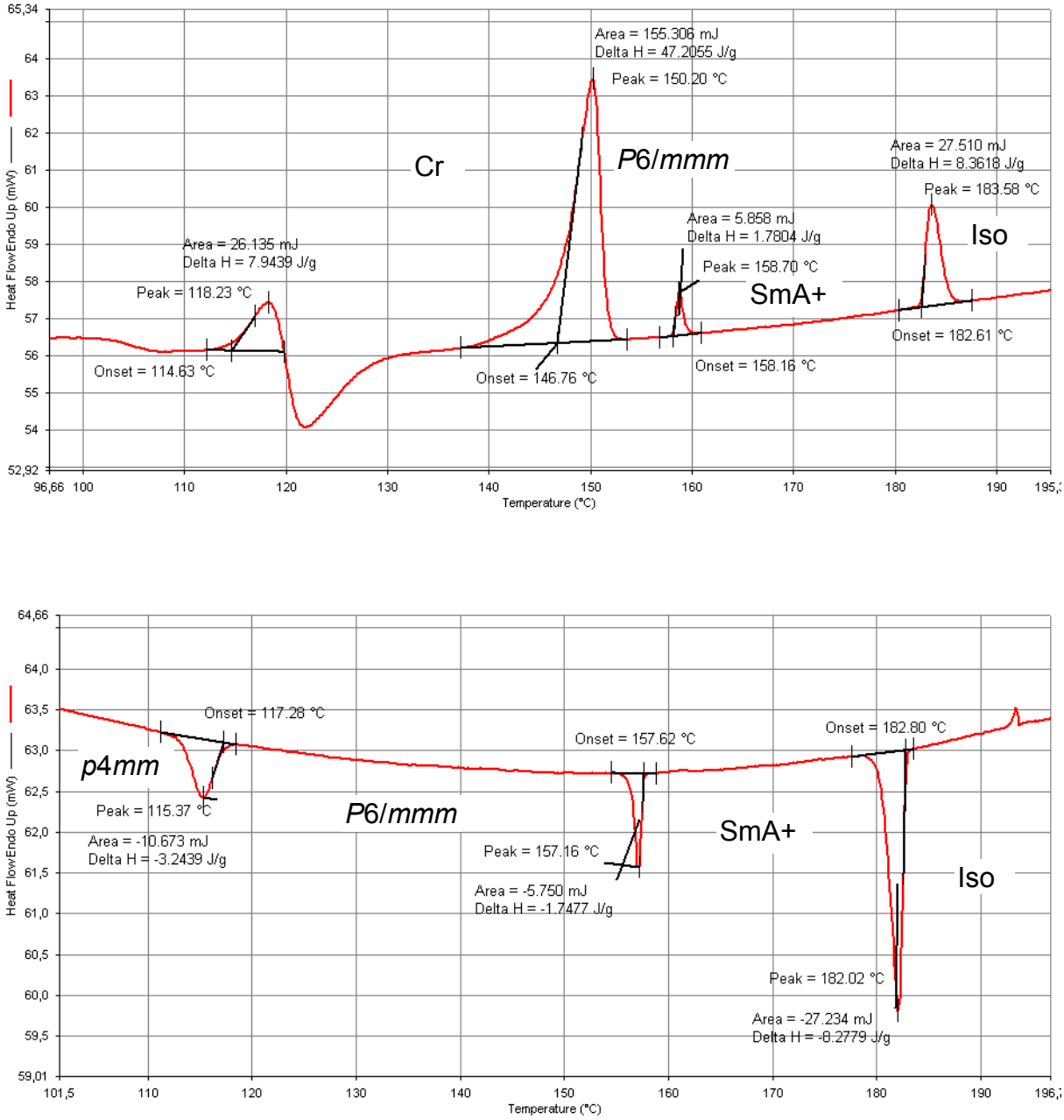

Figure S1e. First DSC heating (top) and cooling scans (bottom) of compound **A10** at 10 K min^{-1}.

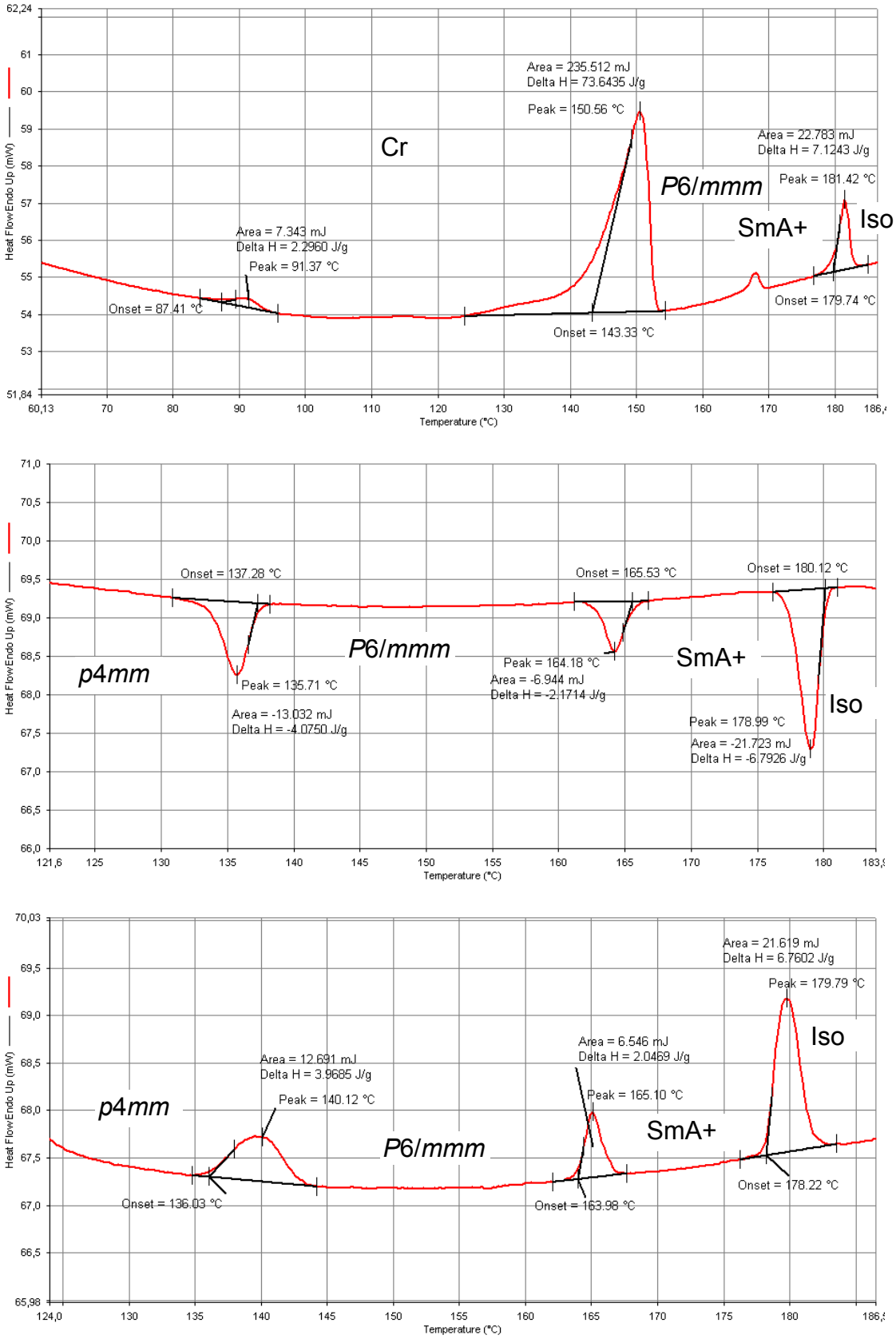

Figure S1f. DSC first heating (top), first cooling (middle) and second heating scans of compound **A11** at 10 K min^{-1}.

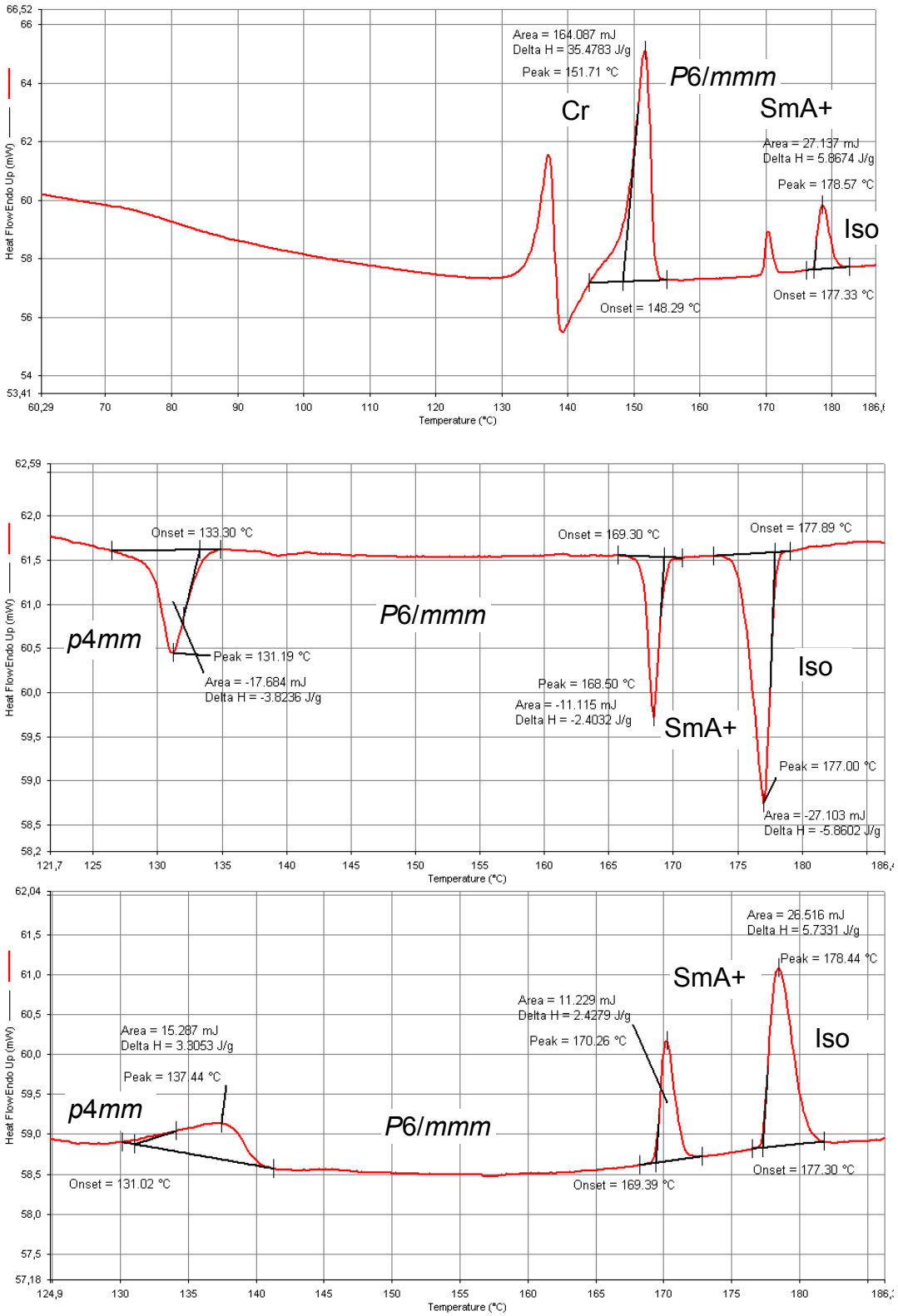

Figure S1g. DSC first heating (top), first cooling (middle) and second heating scans of compound **A12** at 10 K min^{-1}.

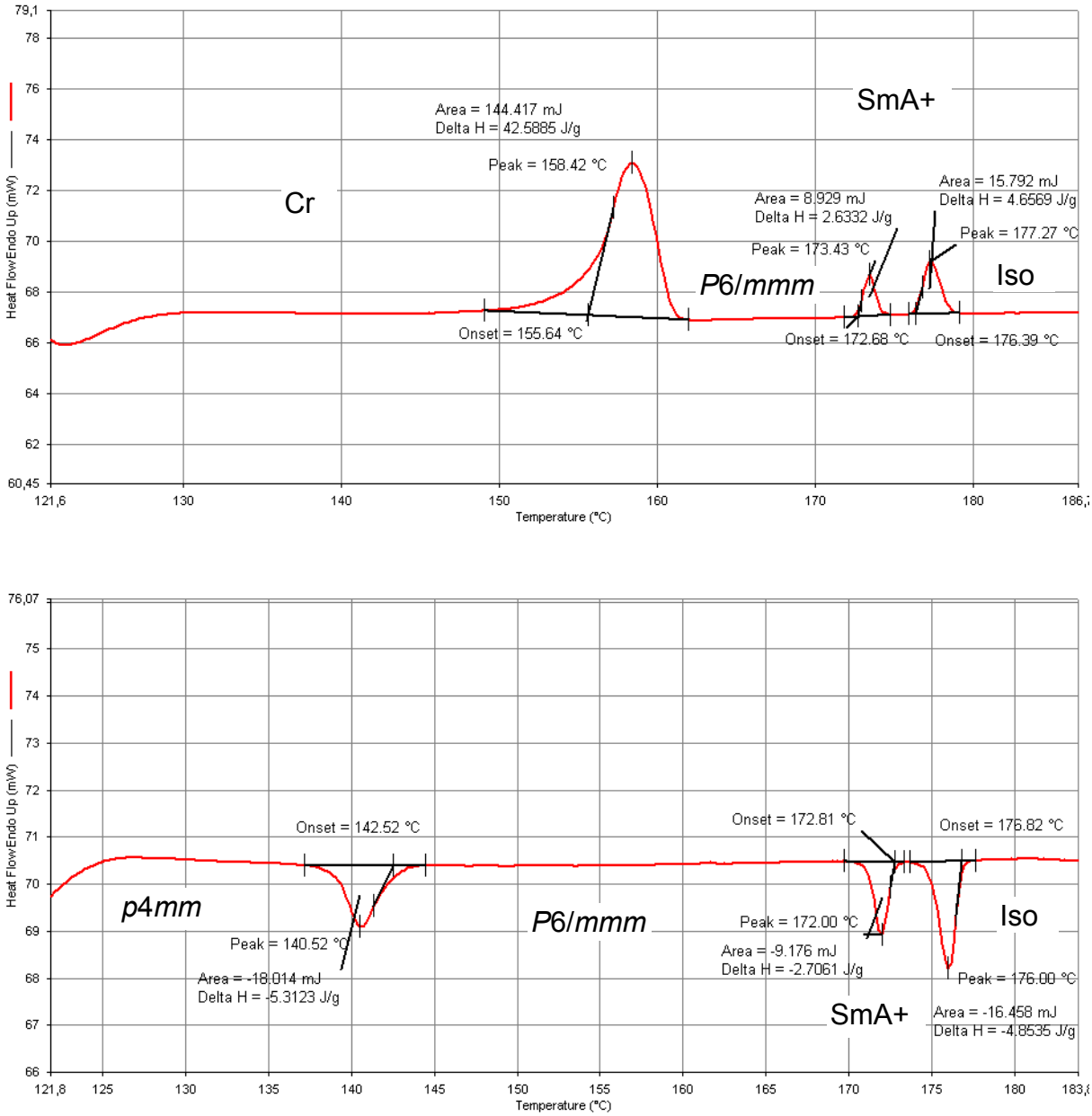

Figure S1h. Second DSC heating (top) and cooling scans (bottom) of compound **A13** at 10 K min^{-1}.

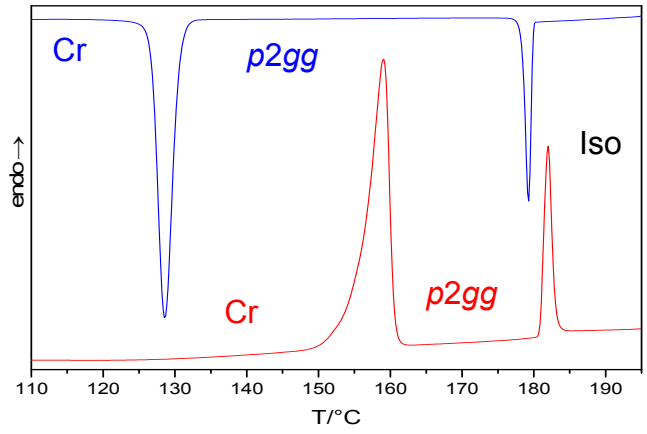

Figure S1i. First DSC heating (red) and cooling scans (blue) of compound **A14** at 10 K min^{-1}.

2.2 Additional textures

2.2.1 Compound A11

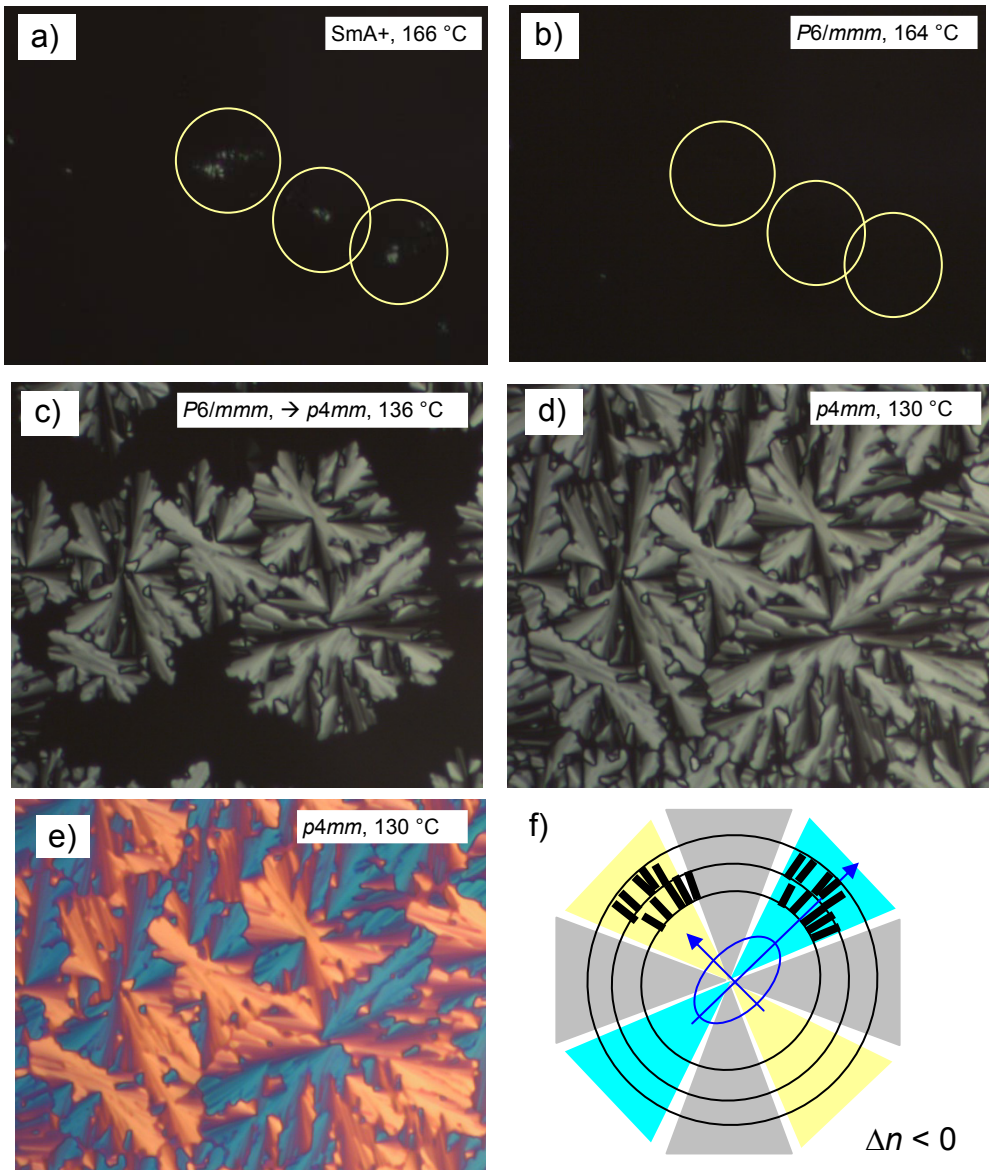

Figure S2. Phase transitions observed in a homeotropic sample surfaces (terphenyls perpendicular and the layer planes parallel to the surface) of **A11**. a) The homeotropic aligned SmA+ phase appears dark with some defects; b) the birefringent defects have disappeared after transition to *P*6/*mmm*; c) the transition to the *p*4*mm* phase is associated with the development of a weakly birefringent spherulitic texture; d) shows the fully developed *p*4*mm* phase. The development of birefringence indicates that the evolving *p*4*mm* lattice has a different direction with respect to the previous hexagonal lattice in *P*6/*mmm*. Hence, the *p*4*mm* lattice develops perpendicular to the hexagonal lattice, i.e. the lipophilic columns become organized parallel to the surfaces at the *P*6/*mmm* – *p*4*mm* transition. Around the lipophilic columns the terphenyls are tangentially aligned and form square cylinders with the vertices (the columns of the hydrogen bonding glycerols) being pinned to the surface (edge-on-surface, see Fig. S3b). This provides an anticlinic 90° tilt between the p-terphenyls, explaining the relatively low birefringence of the homeotropic texture in d). e) Texture of the Col_{squ}/*p*4*mm* phase with λ-retarder plate and f) model showing the organization of the p-terphenyl rods with respect to the indicatrix of the λ plate. The high index axis of the λ plate

is 45° SW to NE. The soft square honeycombs form circles with a defect in the center. The blue shift in the direction of the high index axis of the retarder plate indicates negative birefringence, i.e. the orientation of the π-conjugated rods is perpendicular to the long axes of the prismatic cells, thus confirming a tangential-rod-honeycomb LC structure of the *p*4*mm* phases.

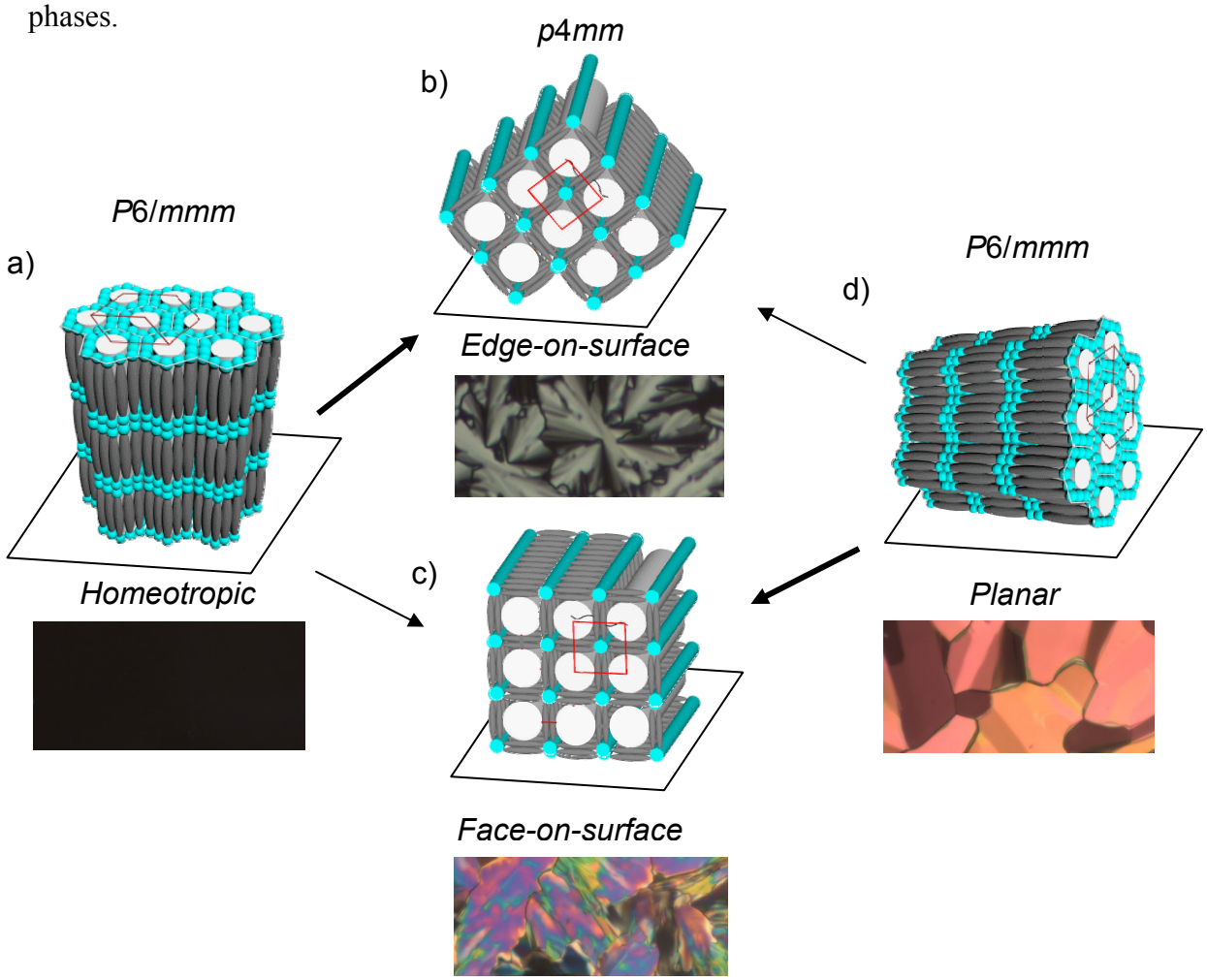

Figure S3. Models showing the alignment of compounds **A*n*** in the three LC phases depending in the mode of alignment and the molecular reorganization at the phase transitions: a) Alignment of the molecules in the homeotropic sample of the *P*6/*mmm* phase of **A11** and b,c) distinct modes of alignment in the *p*4*mm* phase developing on cooling, b) edge-on-surface and c) face-on-surface. d) Alignment of the molecules in a planar sample of the *P*6/*mmm* phase. The higher birefringence of the *p*4*mm* phase obtained in the planar samples d) compared to the homeotropic samples a) suggests that in the first case the formation of the face-on-surface alignment c) and in the second case the edge-on-surface organization b) is preferably formed. Both modes of alignment can be observed in the GISAXS experiments (see Fig. S11c, red lattice = face-on arrangement and yellow lattice = edge-on arrangement). In the homeotropic alignment a) all rods are perpendicular to the surface and therefore $\Delta n = 0$ if viewed perpendicular to the surface. In the highly birefringent texture of the planar aligned *P*6/*mmm* phase in d) the aromatics are parallel to the surface and therefore Δn has maximum value. In this alignment the transition from *P*6/*mmm* to the *p*4*mm* square honeycomb leads to a reduction of the birefringence (orange via green to blue in c)), because half of the molecules become aligned perpendicular to the surface, and these molecules do not significantly contribute to the observed birefringence. For arrangement c) the birefringence is higher than in b) because half of the molecules retain their organization parallel to the surfaces, whereas

in b) the organization of the π-conjugated rods is anticlinic with 90 ° angles, which is known to leads to a very small birefringence.[S1]

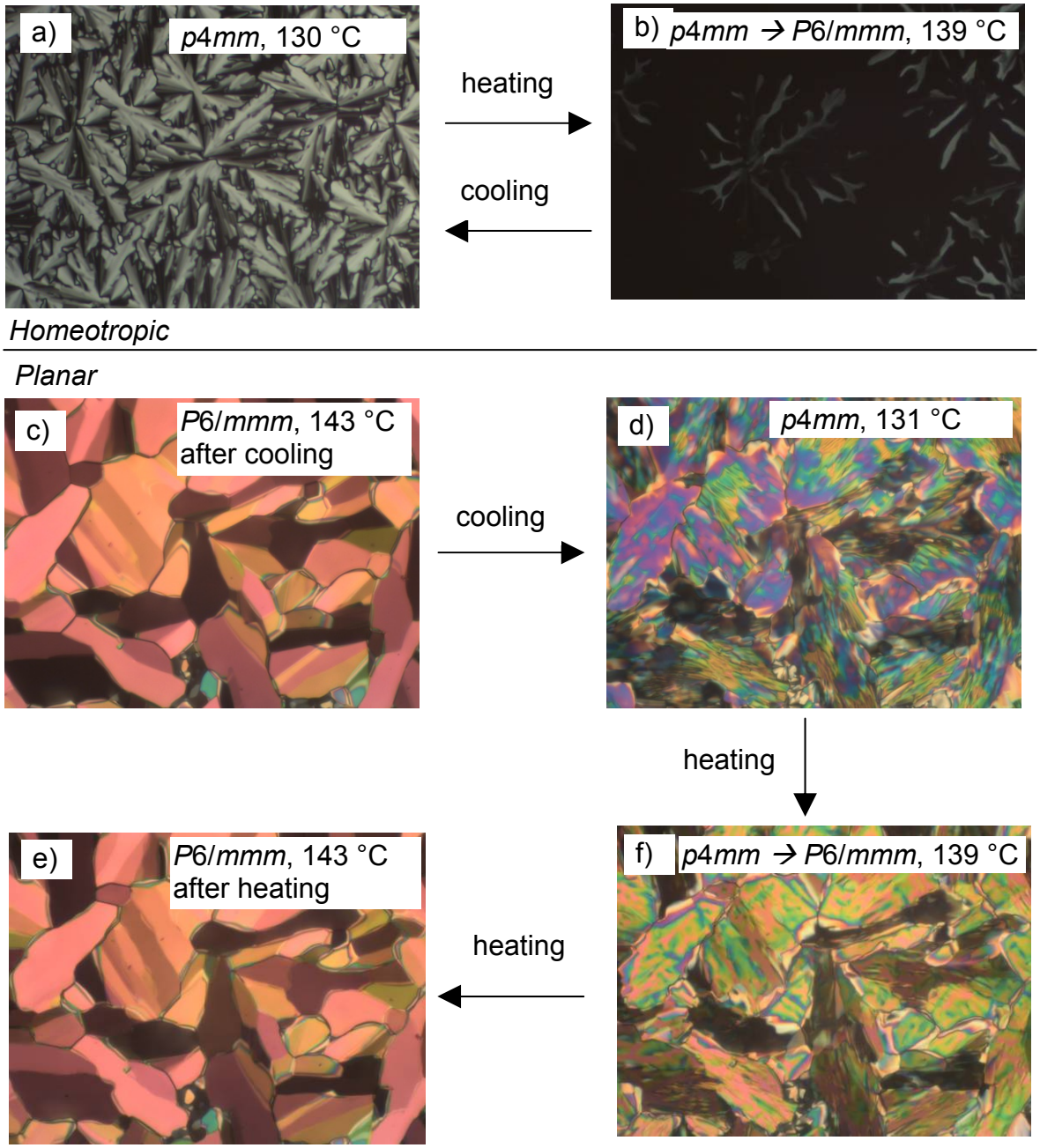

Figure S4. Reversibility of the *P*6/*mmm* - *p*4*mm* phase transition of compound **A11** a,b) in homeotropic alignment and c-f) in planar alignment. The *P*6/*mmm* - *p*4*mm* phase transitions are fully reversible, i.e. there is no temperature hysteresis (see DSCs in Fig. S1f-h) and for both modes of alignment the same textures as observed before the phase transition on cooling were reproducibly restored upon heating.

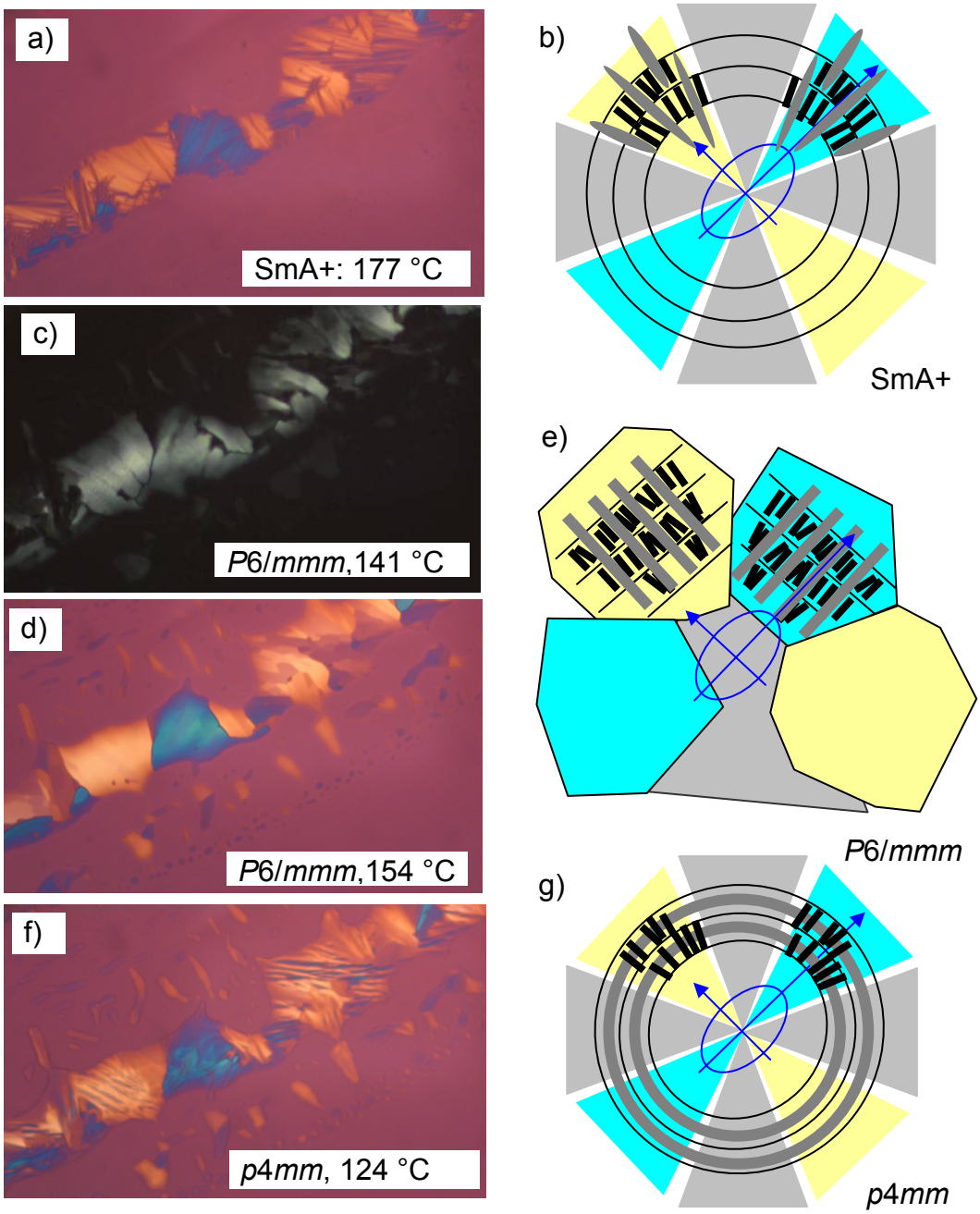

Figure S5. a,c,d,f) Texures observed for a non-covered thin film of **A11** in planar alignment (see also the insets in Fig. 2a-c) and b,e,g) models of azimutal molecular organization (top view on the surface with indicatrix orientation and color shift of the differently aligned regions); a,b) soft layers of the SmA+ phase; c-e) rigid mosaic-like domains of the *P*6/*mmm* phase and f,g) soft columns in the *p*4*mm* phase. The indicatrix orientation of the λ plate is shown in blue; the dark gray lines/circles indicate the columns of the lateral alkyl chains. The majority of blue shifted areas remain blue shifted and the yellow shifted remain yellow shifted during all three phase transition. This means that in planar alignment the azimutal orientation of the aromatic cores, i.e. the direction of the terphenyls, does not change during the two phase transitions. This means that at the *P*6/*mmm*-*p*4*mm* phase transition the alkyl chain columns change their direction by 90°, which requires a disruption of these columns, followed by rebuilding in the perpendicular direction (e → g).

2.2.2 Compound A14

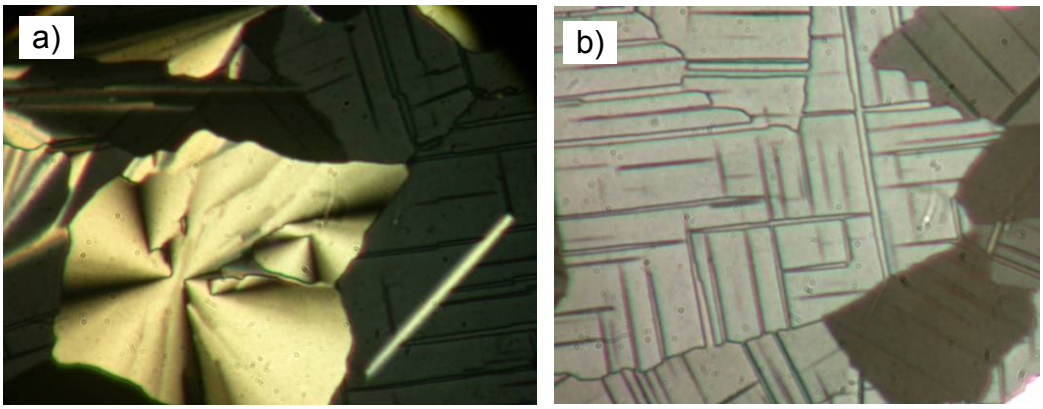

Figure S6. Textures of the *p*2*gg* phase of **A14** at T = 160 °C showing the spherulitic texture (planar aligned regions) and the mosaic texture with stripe pattern in the homeotropic aligned sample.

2.3 Additional XRD data

2.3.1 Compound A5

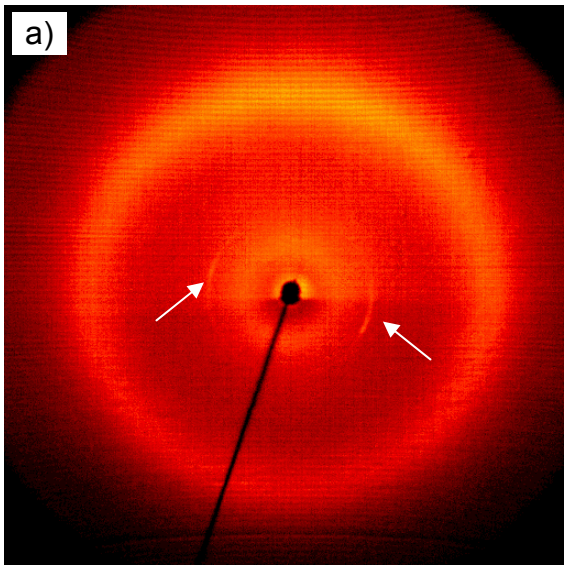

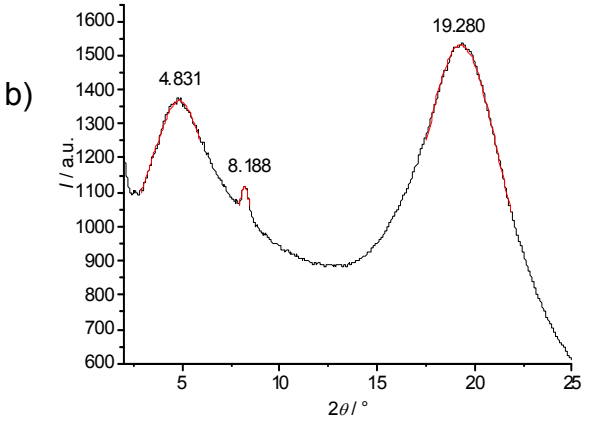

2θ/°	θ/°	d/nm	*hk*
4.831	2.416	1.829	diff
8.188	4.094	1.080	02
19.280	9.640	0.460	diff

Figure S7. 2D-XRD pattern of an aligned sample of the SmA+ phase of **A5** at T = 170 °C. a) original pattern and b) θ-scan over this pattern with numerical data. The diffuse scattering in the small angle range (d = 1.83 nm) has an almost isotropic distribution, whereas the maximum of the diffuse wide angle scattering (d = 0.46 nm) has its maximum perpendicular to the direction of the layer reflection (arrows, (02) reflection, (01)-reflection is not visible; d = 2.16 nm). This indicates a strongly distorted layer structure with short range order between the domains involving the alkyl chains. These domains are small and apparently do not form columns penetrating the layers. The uniform distribution of the diffuse small angle scatteing suggeststs the presence of small almost spherical domains.

2.3.2 Compound A8

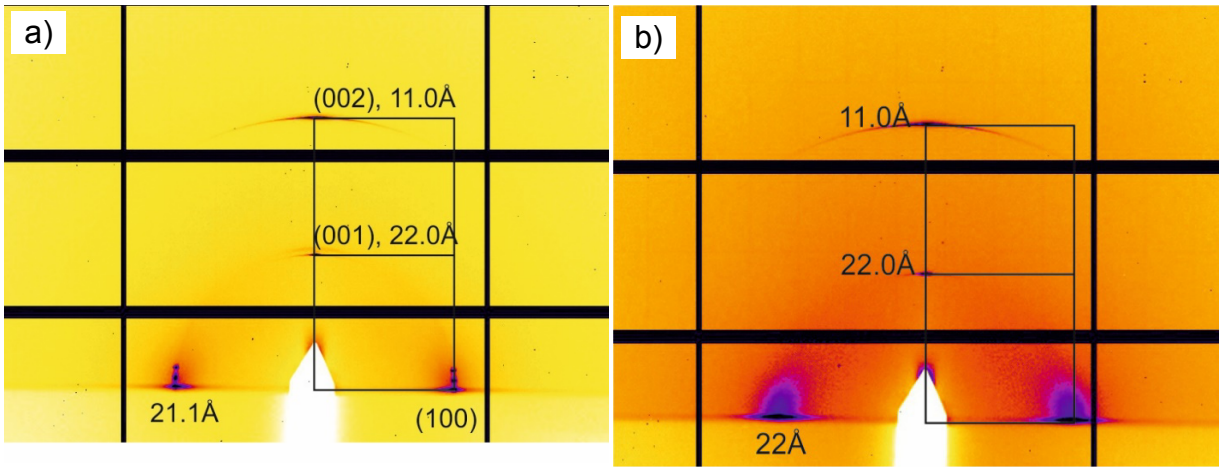

Figure S8. GISAXS patterns of compound **A8** a) in the *P*6/*mmm* phase at 110 °C and b) in the SmA+ phase at 130 °C, showing the diffuse scattering on the equator in b) coalescing to the bragg peaks in a).

2.3.3 Compound A9

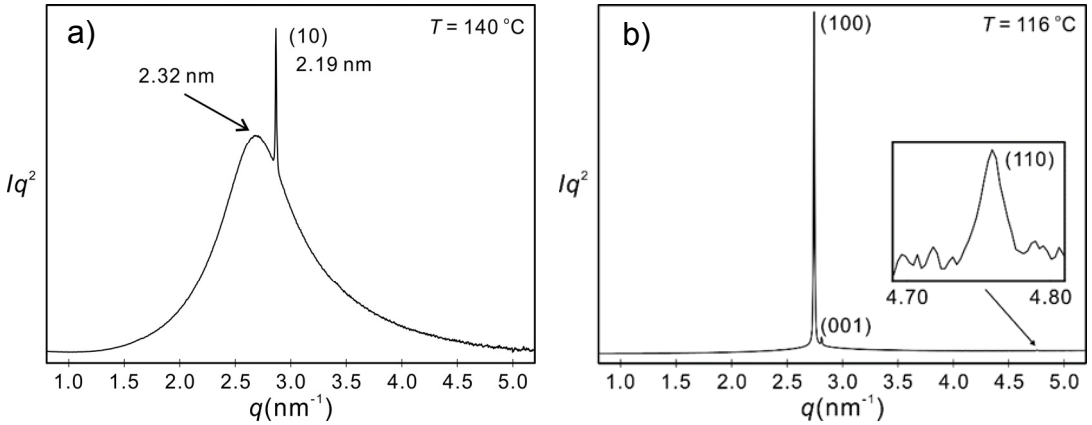

Figure S9. SAXS diffractogram of **A9**: (a) SmA+ phase at 140 °C; (b) the *P*6/*mmm* phase at 116 °C.

Table S2. Experimental and calculated *d*-spacings and relative integrated intensities, for the SmA+ phase of **A9** at 140 ºC and the *P*6/*mmm* phase at 116 ºC. All intensities values are Lorentz and multiplicity corrected.

(*hk*)	$d_{obs.}$- spacings (nm)	$d_{cal.}$- spacings (nm)	Intensity	Phase
(10)	2.19	2.19	100.0	/
	2.32			
d = 2.18 nm, d_2 = 2.32 nm				
(100)	2.29	2.29	100	0
(001)	2.23	2.23	4.7	0
(110)	1.32	1.32	0.2	0
a = 2.64 nm, c = 2.23 nm				

2.3.4 Compound A10

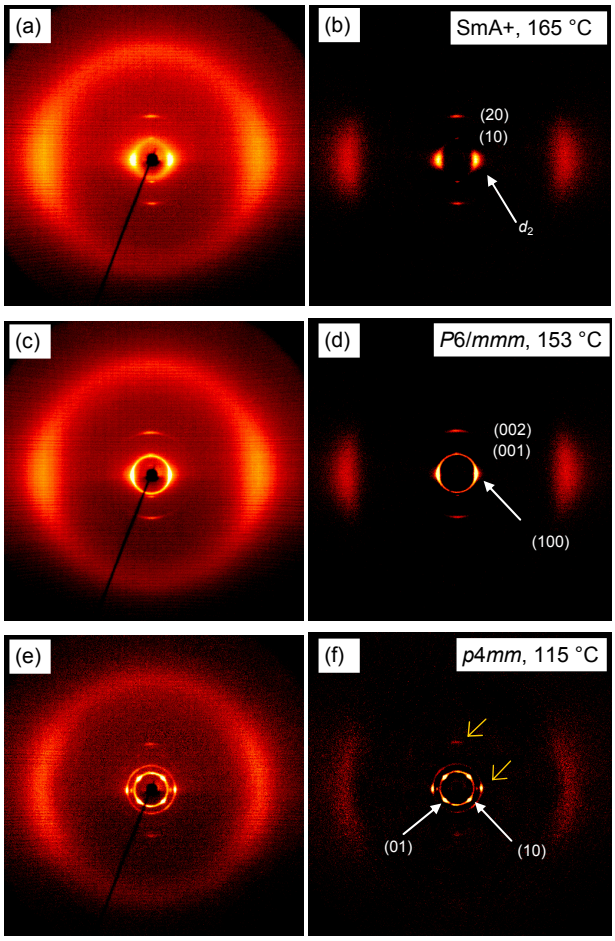

Figure S10. a-f) XRD patterns of an aligned sample of compound **A10** in the distinct LC phases at the indicated temperatures; a,c,e) are the original diffraction patterns; b,d,f) were obtained after subtraction of the scattering pattern in the isotropic liquid state; the yellow arrows in f) indicate the residual diffraction peaks from the *P*6/*mmm* phase.

Table S3. Numerical XRD data of the LC phases of compound **A10** (for diffraction patterns, see Figs. 3 and S10).

a) SmA^+ phase at $T = 165$ °C ($d = 2.13$ nm)

2θ/°	θ/°	d/nm	*hk*
3.519	1.760	2.511	diff
4.148	2.074	2.130	10
8.215	4.108	1.076	20
19.431	9.716	0.457	diff

b) *P*6/*mmm* phase at $T = 153$ °C ($a_{hex} = 2.84$ nm; $c = 2.17$ nm)

2θ/°	θ/°	d_{obs}/nm	*hk*	d_{calc}/nm	d_{obs}-d_{calc}
3.586	1.793	2.464	100	2.460	0.00
4.068	2.034	2.172	001	2.170	0.00
8.049	4.025	1.098	002	1.085	0.01
19.590	9.7925	0.453	diff	-	-

c) *p4mm* phase at T = 115 °C (a_{squ} = 2.81 nm)

2θ/°	θ/°	d_{obs}/nm	*hk*	d_{calc}/nm	d_{obs}-d_{calc}
3.146	1.573	2.808	10	2.808	0.00
4.543	2.272	1.945	11	1.9857	0.04
19.679	9.840	0.451	diff	-	-

2.3.5 Compound A11

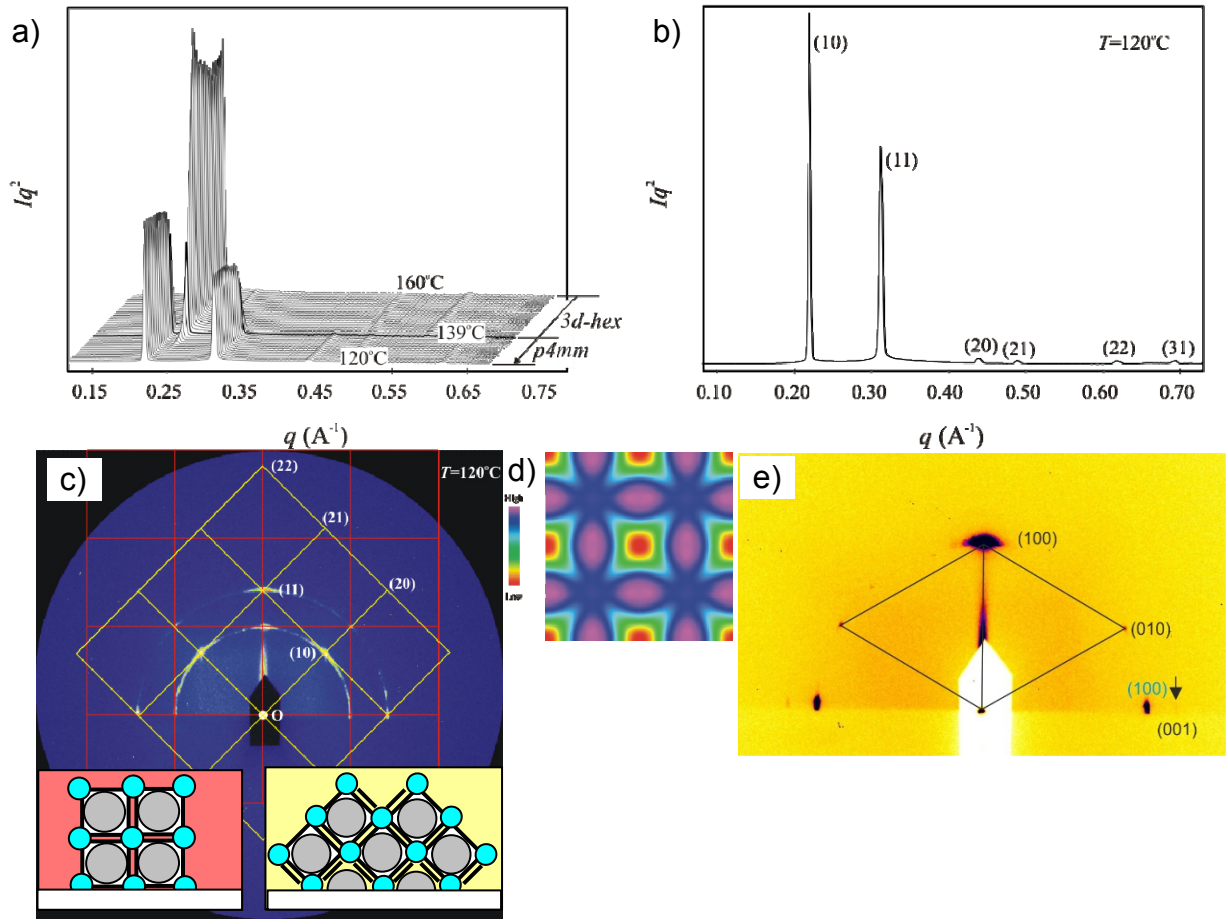

Figure S11. a) Powder pattern showing the temperature dependent development of the small angle scattering pattern of **A11**, b) diffraction pattern in the *p4mm* phase at 120 °C, c) GISAXS pattern of the *p4mm* phase on a Si surface at 120 °C; the insets show the two distinct modes of alignment (see also Fig. S3b); d) reconstructed electron density map of the the *p4mm* phase (from data in Table S4) and e) GISAXS pattern of the *P6/mmm* phase at 150 °C.

Table S4. Experimental and calculated *d*-spacings of the observed SAXS reflections of the square phase *p*4*mm* in compound **A11** at 120 ºC. All intensities values are Lorentz corrected with correction for multiplicity.

(*hk*)	$d_{obs.}$ –spacing (nm)	$d_{cal.}$ –spacing (nm)	*intensity*	*phase*
(10)	2.86	2.86	100.0	π
(11)	2.01	2.02	87.6	π
(20)	1.43	1.43	2.5	π
(21)	1.28	1.28	0.8	π
(22)	1.02	1.01	1.6	0
(31)	0.91	0.90	0.5	0
a_{squ} = 2.86 nm				

2.3.6 Compound A12

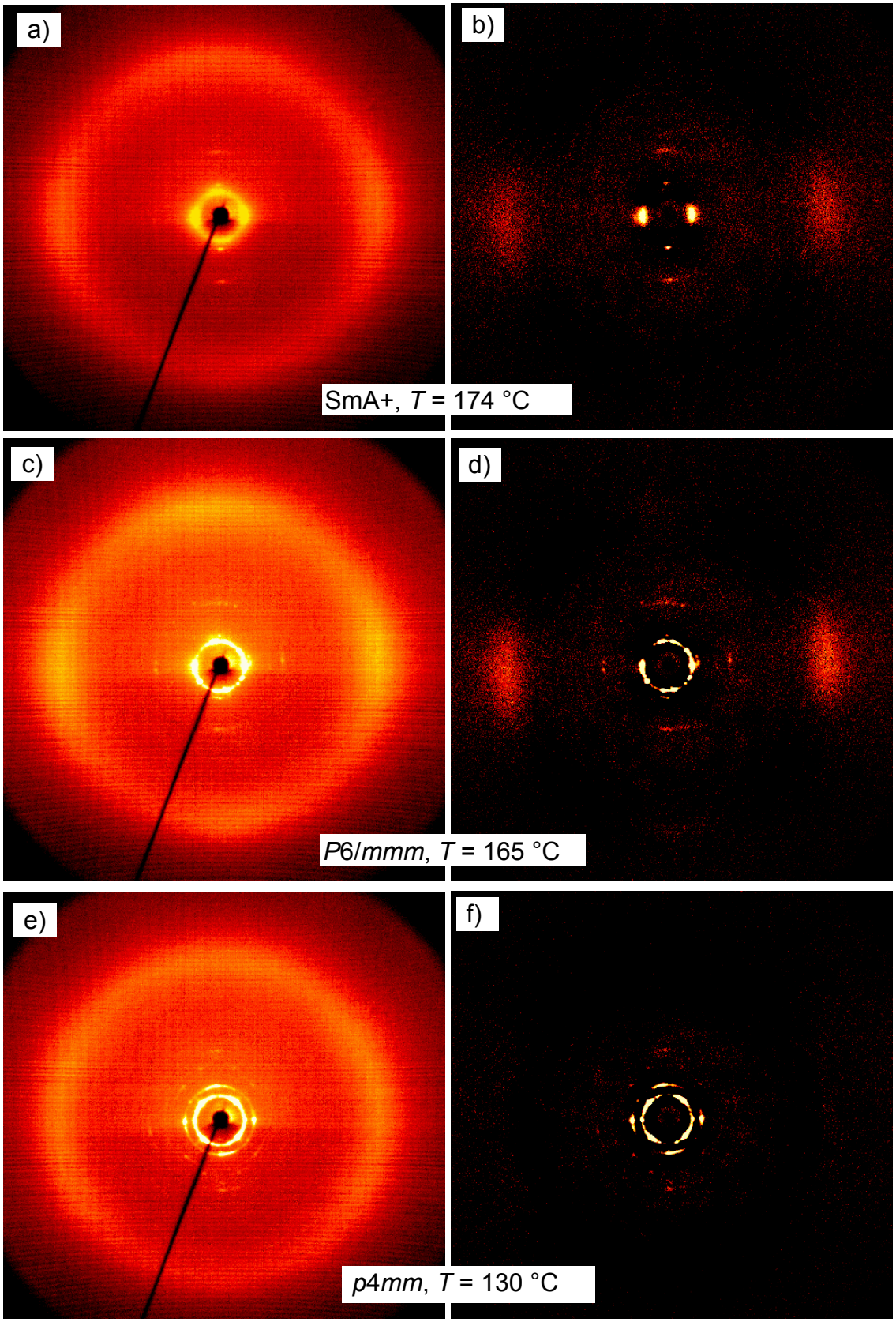

Figure S12. 2D XRD patterns of an aligned sample of compound **A12** in the distinct LC phases at the indicated temperatures; a,c,e) are the original diffraction patterns; b,d,f) were obtained after subtraction of the scattering pattern in the isotropic liquid state.

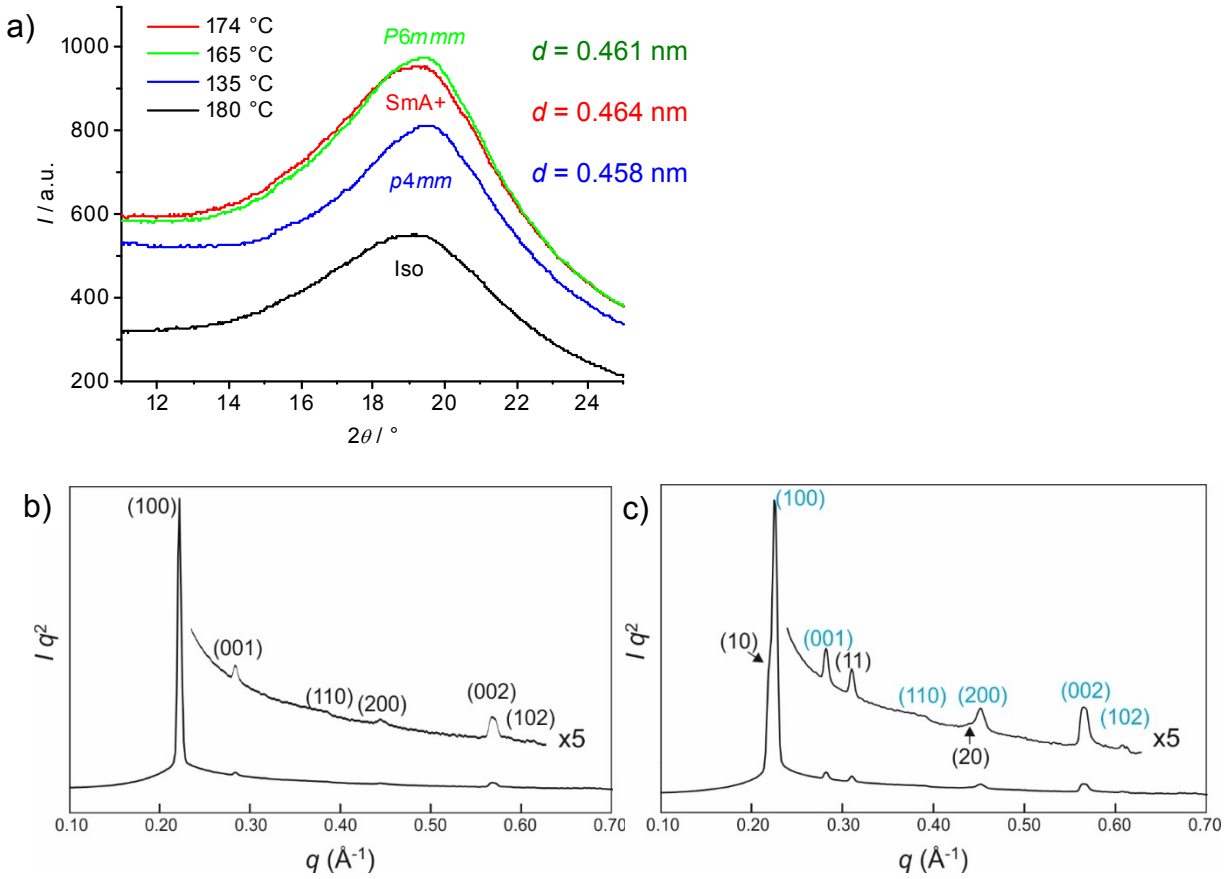

Figure S13. a) WAXS profiles on the distinct LC phases of compound **A12** and b) SAXS pattern of the *P*6/*mmm* phase at 160 °C and c) of the *p*4*mm*+*P*6/*mmm* range at 125 °C .

Table S5. Numerical XRD data of the LC phases of compound **A12**.

*P*6/*mmm* phase at 160 °C (a = 3.27 nm, c = 2.21 nm).

d-exp (nm)	*d*-calc	(*hkl*)	Intensity
2.83	2.83	(100)	100
2.21	2.21	(001)	1.07
1.65	1.63	(110)	0.39
1.41	1.42	(200)	0.77
1.10	1.11	(002)	3.16
1.03	1.03	(102)	0.14

*p*4*mm* phase at 125 °C (a_{squ} = 2.86 nm)

d-exp (nm)	*d*-calc	(*hkl*)	Intensity
2.86	2.86	(10)	100
2.02	2.02	(11)	4.42
1.43	1.43	(20)	1.41

2.3.7 Compound A13

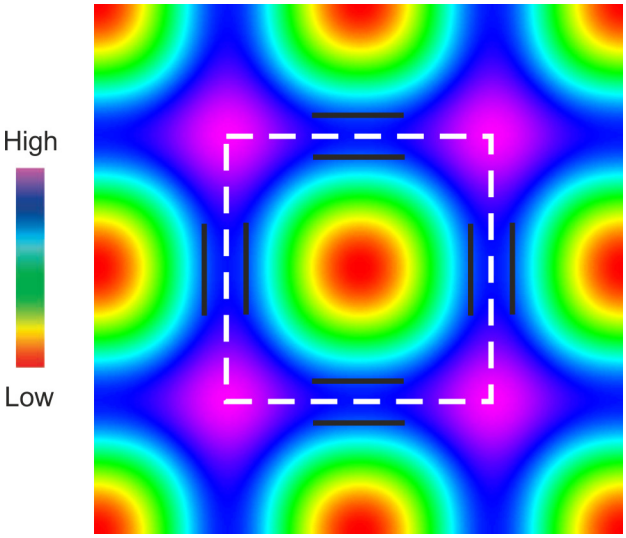

Figure S14. Reconstructed ED map of the Col_{rec}/*p*4*mm* phase of **A13** at 130 °C using the data in Table S6b (black lines represent aromatics).

Table S6. Numerical XRD data of the LC phases of compound **A13**.

a) *P*6/*mmm* phase at 145 °C (a = 3.28 nm, c = 2.20 nm)

d-exp (nm)	*d*-calc (nm)	(*hkl*)	Intensities
2.84	2.84	(100)	100
2.21	2.20	(001)	1.63
1.64	1.64	(110)	0.23
1.42	1.42	(200)	0.42
1.10	1.10	(002)	0.37

b) *p*4*mm* phase at 130 °C (a = 2.83 nm)

d-exp (nm)	(*hk*)	*d*-calc (nm)	Intensities (phases)
2.82	(10)	2.83	100 (-)
2.02	(11)	2.00	8.31 (-)
1.41	(20)	1.42	0.45 (+)

2.3.8 Compound A14

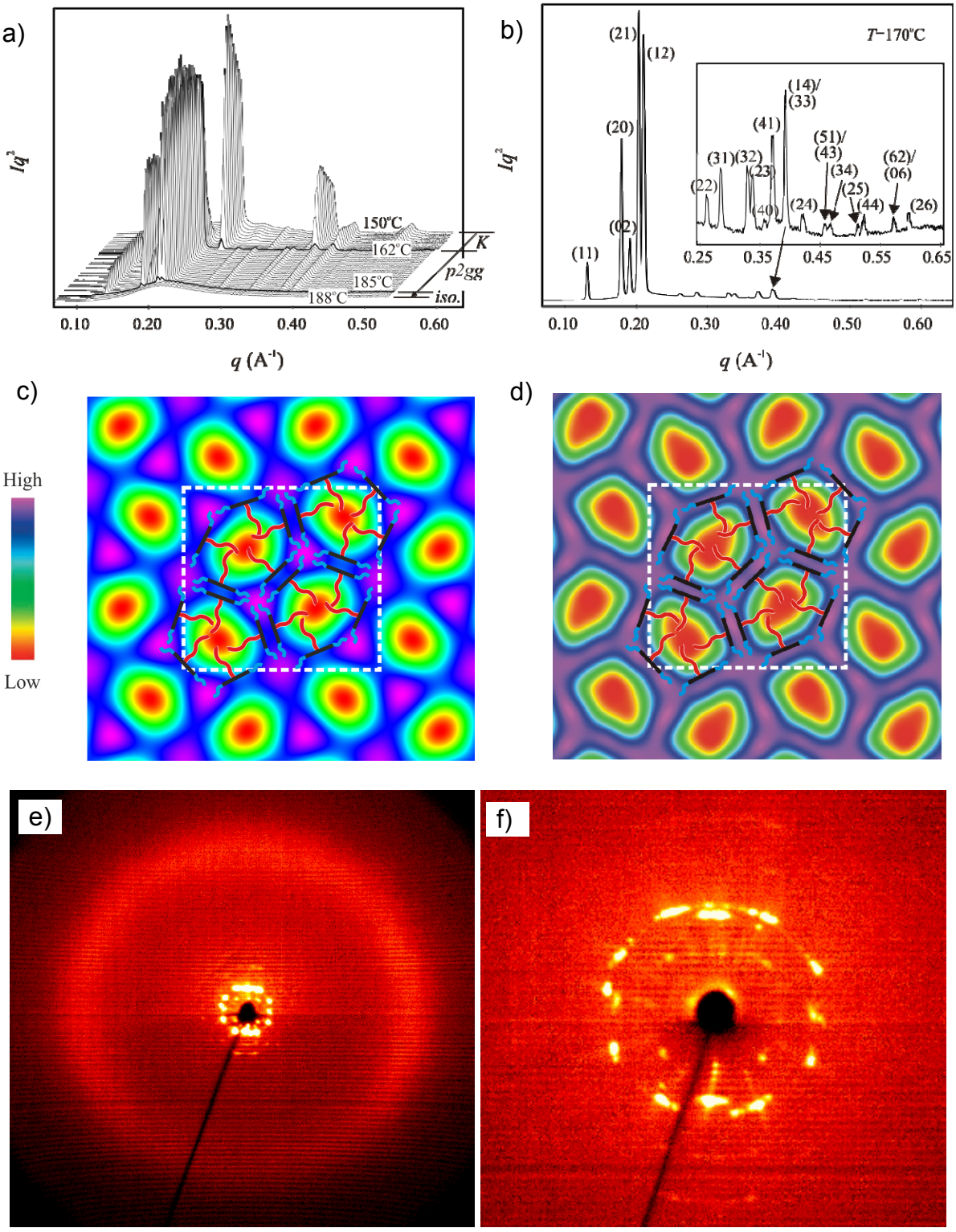

Figure S15. Diffraction patterns of **A14**. a) Temperature scan on cooling and b) diffraction pattern of the *p*2*gg* phase at 170 °C; c) reconstructed electron density map of the *p*2*gg* phase by using the first five diffractions and d) using all reflections (Table S8); e,f) 2D XRD pattern of an aligned sample of the *p*2*gg* phase at T = 175 °C; e) WAXS (maximum of diffuse scattering at d = 0.47 nm) and f) SAXS pattern at T = 120 °C.

Table S7. Experimental and calculated *d*-spacings of the observed SAXS reflections (Fig. 15b; synchrotron source) of the rectangular *p*2*gg* phase in compound **A14** at 170 ºC. All intensities values are Lorentz corrected with correction for multiplicity.

(*hk*)	$d_{obs.}$ –spacing (nm)	$d_{cal.}$ –spacing (nm)	*intensity*	*phase*
(11)	4.79	4.79	10.4	π
(20)	3.50	3.50	94.3	0
(02)	3.29	3.29	36.5	0
(21)	3.09	3.09	95.3	π
(12)	2.98	2.98	100.0	π
(22)	2.40	2.40	1.0	0
(31)	2.20	2.20	2.0	0
(32)	1.90	1.90	2.2	0
(23)	1.86	1.86	2.1	0
(40)	1.75	1.75	0.4	0
(41)	1.69	1.69	4.0	π
(33)	1.60	1.60	2.8	0
(14)			2.8	π
(24)	1.49	1.49	0.6	0
(51)	1.37	1.37	0.1	π
(43)			0.1	π
(34)	1.35	1.34	0.5	π
(25)	1.23	1.23	0.1	π
(44)	1.20	1.20	0.5	π
(62)	1.10	1.10	0.1	π
(06)			0.3	π
(26)	1.05	1.05	0.3	π
a = 7.00 nm, b = 6.58 nm				

2.4. Structural parameters

Table S8. Lattice parameters and calculation of the molecular volume (V_{mol}), volume of the unit cells (V_{cell}), number of molecules in these unit cells (n_{cell}) and number of molecules in the lateral cross section of the honeycomb walls (n_{wall}).[a]

Compd.	f_R	Phase	T (°C)	Lattice parameters (nm)	d_{diff} (nm)	V_{cell}	V_{mol} (nm^3)	n_{cell}	n_{wall}
A5	*0.20*	SmA+	170	d_1 = 2.16, d_2 =1.83 [b]	0.46	-	-	-	-
A8	*0.28*	SmA+	130	d_1 = 2.20, d_2 =2.2 [b]	0.46	-	-	-	-
A8		*P*6/*mmm*	110	a_{hex} = 2.44, c = 2.20	0.45	11.3	0.73	13.9	2.6
A9	*0.31*	SmA+	160	d_1 = 2.19, d_2 =2.32	0.46	-	-	-	-
A9		*P*6/*mmm*	110	a_{hex} = 2.64, c = 2.18	0.45	13.2	0.75	15.7	2.6
A10	*0.33*	SmA+	165	d_1 = 2.13, d_2 = 2.51 [b]	0.46	-	-	-	-
A10		*P*6/*mmm*	153	a_{hex} = 2.84, c = 2.17	0.45	15.5	0.78	17.4	2.7
A10		*p*4*mm*	115	a_{squ} = 2.81	0.45	3.55	0.78	4.1	2.0
A11	*0.35*	SmA+	175	d_1 = 2.16, d_2 = 2.66 [b]	0.47	-	-	-	-
A11		*P*6/*mmm*	155	a_{hex} = 3.05, c = 2.22	0.46	17.9	0.80	20.0	2.7
A11		*p*4*mm*	120	a_{squ} = 2.86	0.45	3.68	0.80	4.1	2.0
A12	*0.37*	SmA+	174	d_1 = 2.14, d_2 = 2.83 [b]	0.46	-	-	-	-
A12		*P*6/*mmm*	160	a_{hex} = 3.27, c = 2.21	0.46	20.5	0.83	22.0	2.7
A12		*p*4*mm*	125	a_{squ} = 2.86	0.46	3.76	0.83	4.0	2.0
A13	*0.39*	SmA+	175	d_1 = 2.12, d_2 = 2.84	0.46	-	-	-	-
A13		*P*6/*mmm*	145	a_{hex} = 3.28, c = 2.20	0.46	20.5	0.85	21.5	2.7
A13		*P*4*mm*	130	a_{squ} = 2.83	0.46	3.68	0.85	3.9	1.9
A14	*0.41*	*p*2*gg*	115	a = 7.00, b = 6.58	0.47	21.6	0.88	22.0	2.2

[a] f_R = volume fraction of the lateral alkyl chain; $V_{cell} = A_{cell} \times h$, where $A_{cell} = a_{aqu}^2$ for *p*4*mm*, and $a \times b$ for the rectangular phases; for the tangential-rod-honeycombs h corresponds to the d-value of the maximum of the diffuse wide angle scattering (d_{diff}). For the *P*6/*mmm* phases $V_{cell} = A_{cell} \times c$ (with $A_{cell} = \sqrt{3}/2 \times a_{hex}^2 = 0.866\ a_{hex}^2$); V_{mol} = volume for a single molecule as calculated using crystal volume increments;[S2] n_{cell} = number of molecules in the unit cell, calculated according to $n_{cell} = k \times V_{cell}/V_{mol}$ with k = 0.893, being a correction for the packing density in the LC state;[S3] n_{wall} = average number of molecules in the cross section of the honeycomb walls as calculated for the tangential-rod-honeycombs from n_{cell} by deviding by the number of walls per unit cell (*p*4*mm*: 2, *p*2*gg*: 10) and for the coaxial rod honeycombs (*P*6/*mmm*) according to $n_{wall} = [a_{hex} - (2f_R \times A_{cell}/\sqrt{3})^{1/2}]/d_{diff}$; d_{diff} = position of the diffuse wide angle scattering maximum; for details of the calculations, see the following Section 2.5 and Fig. S16. [b] Diffuse small angle scattering.

2.5 Calculation of n_{wall} for the *P6/mmm* phases

The volume of the alkyl chains in each unit cell (V_R) is the unit cell volume (V_{cell}) multiplied by the volume fraction of the lateral chains (f_R):

$$V_R = V_{cell} \times f_R = A_R \times c = A_{cell} \times c \times f_R \quad (1)$$

divison by parameter c gives the corresponding areas:

$$A_R = A_{cell} \times f_R \quad (2)$$

Where A_R is the area of the lateral chains in each hexagonal 2d unit cell; A_{cell} is calculated from a_{hex} by: $A_{cell} = \sqrt{3}/2 \times a_{hex}^2$, and similarly, the area required by the alkyl chains A_R is calculated by $A_R = a_R^2 \times \sqrt{3}/2$ and therefrom it follows after transposition that

$$a_R = (2A_R/\sqrt{3})^{1/2} \quad (3)$$

(for definition of a_R, see Fig. S16a) replacing A_R by equ. (2) gives

$$a_R = (2f_R \times A_{cell}/\sqrt{3})^{1/2} \quad (4)$$

The thickness of the aromatic walls d_{wall} is the difference $d_{wall} = a_{hex}\text{-}a_R$ and according to equ (4):

$$d_{wall} = a_{hex}\text{-}a_R = a_{hex}\text{-} (2f_R \times A_{cell}/\sqrt{3})^{1/2} \quad (5)$$

d_{wall} divided by the average distance between the rotationally disordered aromatics, (position of the maximum of the diffuse wide angle scattering d_{diff}) gives the approximate number of molecules in the lateral cross section of the walls (the walls between two prismatic cells of the alkyl chains; the number of molecules in the diameter of shell around a single R_H column is $n_{wall}/2$) in the hexagonal coaxial-rod-honeycombs (n_{wall}) according to:

$$n_{wall} = d_{wall}/d_{diff} = [a_{hex} - (2f_R \times A_{cell}/\sqrt{3})^{1/2}]/d_{diff} \quad (6)$$

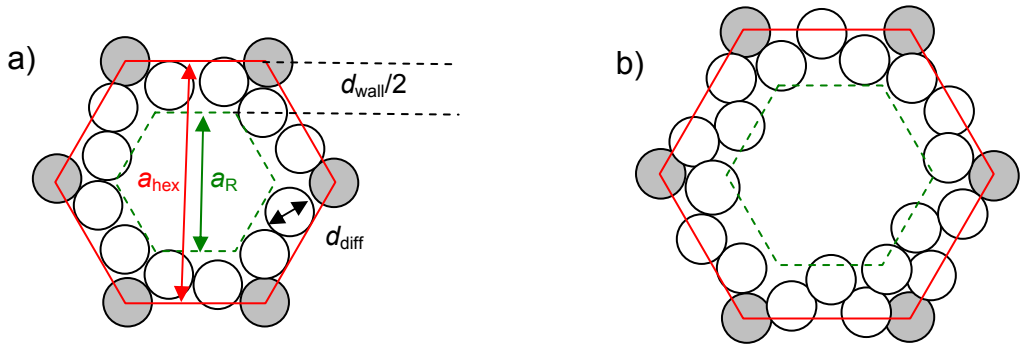

Figure S16. Cross section through one coaxial hexagonal honeycomb of the *P6/mmm* phases (approximately in scale) of a) compound **A8** and b) compound **A13** with explanation of the dimensions used for calculations and the arrangement of 14 (12 white and 2 gray), and 21 (19 white and 2 gray) molecules per unit cell, respectively, leading to n_{wall} = ~2.6-2.7; ($d_{wall}/2$ ~1.3 molecules). The circles represent the cross sections through the preferably edge-to-face

organized and rotationally disordered terphenyls; each of the gray circles at the vertices is shared by three cells; the interior in the green dashed hexagon is filled by the alkyl chains.

2.6 Molecular models and MD simulations

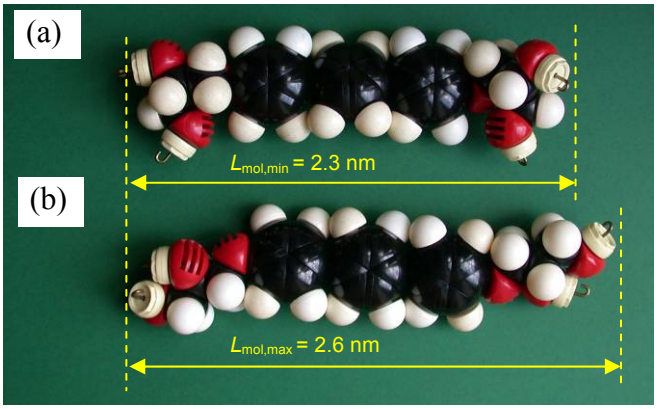

Figure S17. Molecular models showing compounds **A*n*** (without lateral chain) in the conformations with a) minimized and b) maximized molecular length corresponding to $L_{mol,min}$ = 0.23 nm and $L_{mol,max}$ = 0.26 nm, respectively.

Figure S18. Some conformations of compound **A10.**

Figure S19. a) Model of a section of the channel structure in the *P*6/*mmm* phase of **A10** and b) cross section through a square honeycomb cell of **A10** with different modes of prefereed alkyl chain alignment (Fig. S18).

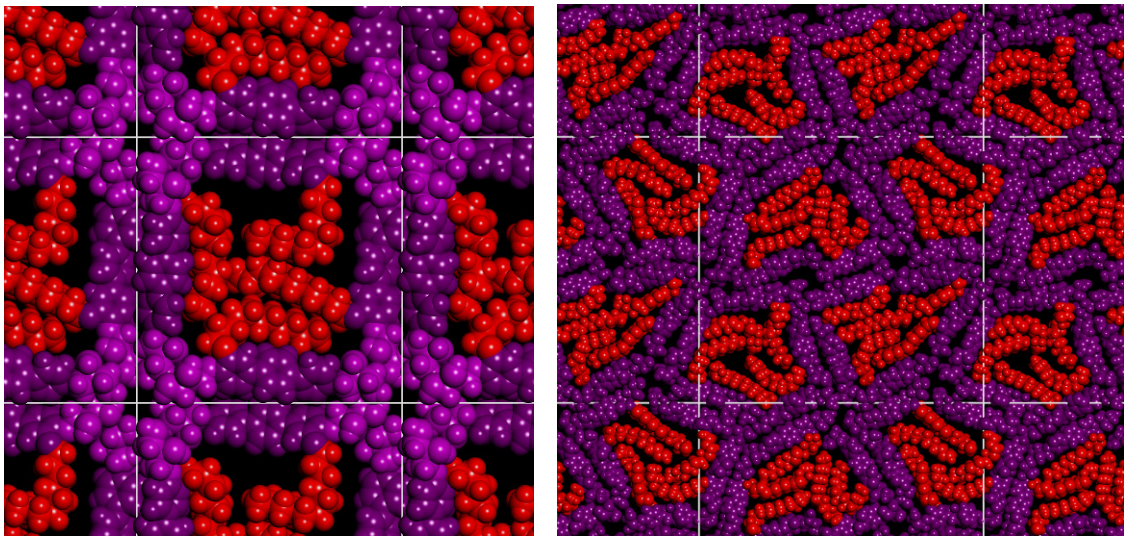

Figure S20. The snapshots of molecular dynamics simulations a) of Col_{squ}/*p*4*mm* phase of compound **A9**, and b) Col_{rec}/*p*2*gg* phase of **A14**; color coding is as follows: red = alkyl chains (lowest electron density), purple = terphenyl and glycerol groups (high density). In both tangential-rod-honeycmbs the preferred orientation of the alkyl chains is parallel to the p-terphenyl cores in the walls.

3. Synthesis and analytical data

3.1 General

Synthesis of the compounds was performed according to Scheme S1 using the procedures described below. Unless otherwise noted, all starting materials were purchased from commercial sources and were used without further purification. Column chromatography was performed with silica gel 60 (63-200 μm, Merck). Determination of structures and purity of intermediates and products was obtained by NMR spectroscopy (VARIAN Gemini 200, Unity 500 and VRX 400, all spectra were recorded at 27 °C) Microanalyses were performed using a CHNS-932 (Leco) elemental analyzer. The purity of all products was checked with thin layer chromatography (silicagel 60 F254, Merck). $CHCl_3$/EtOAc mixtures and $CHCl_3$/MeOH mixtures were used as eluents and the spots were detected by UV radiation or in I_2 vapour. All compounds represent racemic mixtures of diastereomers.

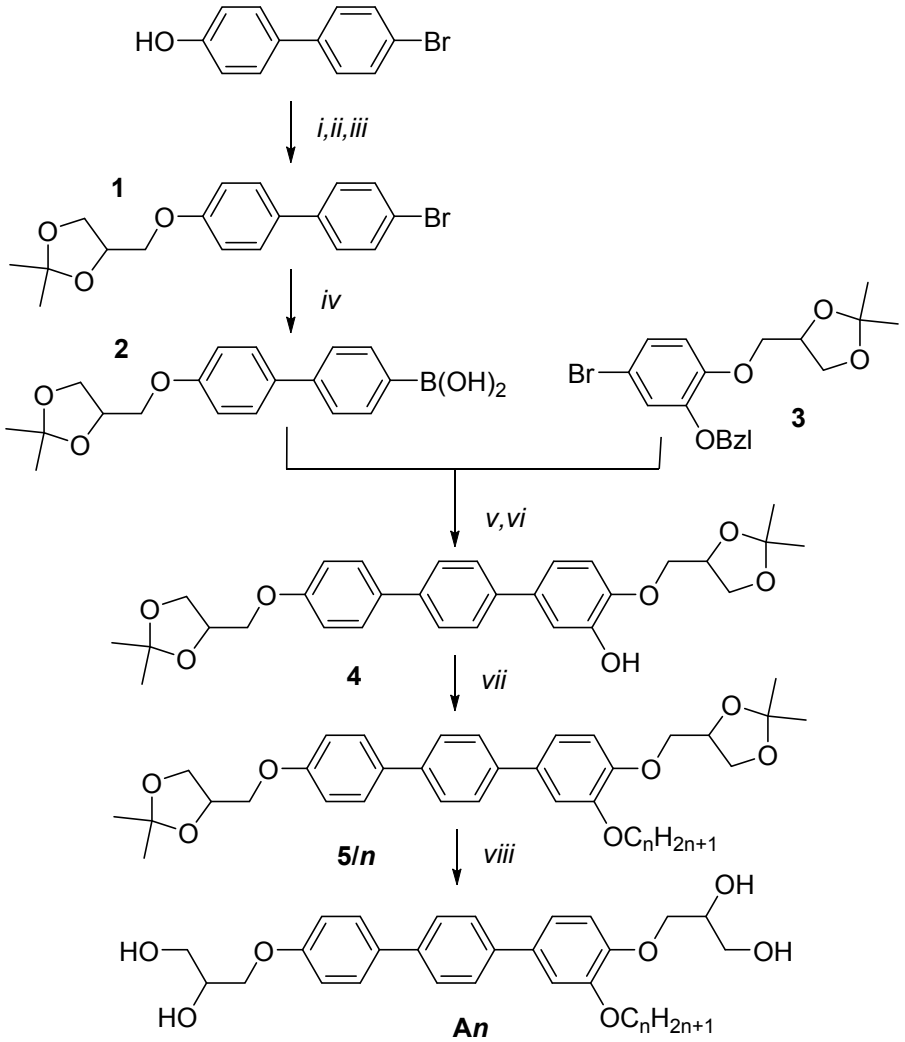

Scheme S1. Synthesis of compounds **A*n***. *Regents and conditions*: i: CH_2=CH-CH_2Br, K_2CO_3, 2-butanone, reflux, 6 h; ii: *N*-methylmorpholine-*N*-oxide (NMMNO), cat. OsO_4, acetone, 20 °C, 60 h;[S4] iii: $Me_2C(OMe)_2$, cat. pyridinium p-toluenesulfonate (PPTS);[S5] iv: 1. *n*-Buli, -85 °C, 2. $B(OMe)_3$, -85→20 °C, 3. $KH_2PO_4/Na_2HPO_4/H_2O$ buffer;[S9] v: cat. $Pd[PPh_3]_4$, $NaHCO_3$, H_2O, glyme, reflux, 5 h;[S6] vi: cyclohexene, cat. $Pd(OH)_2$/C, THF, 20 °C,

14 h;[S7] vii: $C_nH_{2n+1}Br$, K_2CO_3, 2-butanone, reflux, 5h; viii: MeOH, THF, cat. PPTS, reflux, 6-24 h.[8]

n-Alkylbromides (Merck), 4'-bromobiphenyl-4-ol (Merck), trimethylborat (Merck), n-butyllithium 1.6 M in hexane (ACROS), glyme (Alfa Aesar), osmium tetroxide (Berlin Chemie), $Pd(OH)_2$ on charcoal (Fluka), pyridinium-p-toluene sulfonate (Merck) and *N*-methylmorpholine-*N*-oxide 50-wt.% in H_2O (Fluka) were used as received.

4'-[(2,2-Dimethyl-1,3-dioxolane-4-yl)methoxy]benzene-4-boronic acid (3) was prepared as described in ref.[S9]: Colorless solid, mp.: 143-146 °C; ^{1}H-NMR (acetone-D_6, J/Hz, 400 MHz) δ = 7.81 (d, ^{3}J(H,H) = 8.7, 2H, Ar-H), 6.92 (d, ^{3}J(H,H) = 9.5, 2H, Ar-H), 4.44 (m, 1H, OCH), 4.14 (dd, ^{2}J(H,H) = 8.3, ^{3}J(H,H) = 6.4, 1H, OCH_2), 4.09 - 4.02 (m, 2H,OCH_2), 3.85 (dd, ^{2}J(H,H) = 8.3, ^{3}J(H,H) = 6.2, 1H, OCH_2), 1.37 (s, 3H, CH_3), 1.32 (s, 3H, CH_3).

3.2 Synthesis of 4,4''-bis[(2,2-dimethyl-1,3-dioxolane-4-yl)methoxy]-p-terphenyl-3-ol (4)

4-Allyloxy-4'-bromobiphenyl[S10]

A mixture of 4'-bromobiphenyl-4-ol (25 g, 0.10 mol), allyl bromide (12 ml, 0.11 mol) and K_2CO_3 (27.6 g, 0.2 mol) in 2-butanone (250 ml) was stirred for 6 h under reflux. After cooling to room temperature, the reaction mixture was poured into ice-water (250 ml) and extracted with diethyl ether (3 x 100 ml). The combined organic layers were washed with water and brine. After drying over anhydrous Na_2SO_4, filtration and evaporation of the solvent, the crude product was used without further purification. Colorless solid; yield: 28.2 g (0.098 mol, 98 %); mp 124-128 °C; ^{1}H-NMR ($CDCl_3$,J/Hz, 400 MHz) δ = 7.50(d, ^{3}J(H,H) = 8.5, 2H, Ar-H), 7.45 (d, ^{3}J(H,H) = 8.7, 2H, Ar-H), 7.38 (d, ^{3}J(H,H) = 8.5, 2H, Ar-H), 6.96 (d, ^{3}J(H,H) = 8.7, 2H, Ar-H), 6.11 - 6.01 (m, 1H, C*H* = CH_2), 5.42 (dd, ^{2}J(H,H) = 1.5, ^{3}J(H,H) = 17.3, 1H, CH = C*H*$_2$), 5.29 (dd, ^{2}J(H,H) = 1.2, ^{3}J(H,H) = 10.2, 1H, CH = C*H*$_2$), 4.56 (d, ^{3}J(H,H) = 5.2, 2H, OCH_2).

3-(4'-Bromobiphenyl-4-yloxy)propane-1,2-diol

To a mixture of 4-allyloxy-4'-bromobiphenyl (27.9 g , 0.097 mol) in acetone (200 ml) was added NMMO (13.8 g, 0.116 mol of a 50-wt% aq. solution) and OsO_4 (16 ml of a 0.004M solution in *tert*-butanol). The mixture was stirred at room temperature for 60 h and checked by TLC. After addition of saturated Na_2SO_3 solution in water (250 ml), the mixture was stirred for 1 h. The solution was was diluted with water (500 ml) and extracted with Et_2O (3 x 100 ml. The combined organic layers where washed with 10 % aq. H_2SO_4, sat. aq. $NaHCO_3$, water and brine. After drying over anhydrous Na_2SO_4, filtration and evaporation of the solvent, the crude product was crystallized from EtOAc. Colorless solid; yield: 28.4 g (0.088 mol, 91 %), mp.: 178-180 °C; ^{1}H-NMR (DMSO-D_6, J/Hz, 400 MHz) δ = 7.58-7.53 (m, 6H, Ar-H), 6.99 (d, ^{3}J(H,H) = 8.9, 2H, Ar-H), 4.91 (d, ^{3}J(H,H) = 5.0, 1H, OH), 4.62 (t, ^{3}J(H,H) = 5.6, 1H, OH), 4.01 (dd, ^{2}J(H,H) = 9.9, ^{3}J(H,H) = 4.2, 1H, OCH_2), 3.87 (dd, ^{2}J(H,H) = 10.0, ^{3}J(H,H) = 6.2, 1H, OCH_2), 3.78 (m, 1H, C*H*OH), 3.42 (dd, ^{3}J(H,H) = 5.8, ^{3}J(H,H) = 5.6, 2H, OCH_2).

4-(4'-Bromobiphenyl-4-yloxymethyl)-2,2-dimethyl-1,3-dioxolane (1)

A suspension of 3-(4'-bromobiphenyl-4-yloxy)propane-1,2-diol (16.5 g, 0.051 mol) and PPTS (0.1 g, 0.4 mmol) in 2,2-dimethoxypropane (200 ml) was stirred at room temperature for 60 h.

Thereafter, the solvent was evaporated and the residue was taken up in diethyl ether. The solution was washed with sat. aq. $NaHCO_3$, water and brine. After drying over anhydrous Na_2SO_4, the solvent was removed under reduced pressure and the crude product was purified by crystallization from $CHCl_3$ /n-hexane. Colorless solid; yield: 14.9 g (0.041 mol, 81 %); mp.:103-106 °C; ^{1}H-NMR ($CDCl_3$, J/Hz, 400 MHz) δ = 7.51 (d, ^{3}J(H,H) = 8.5, 2H, Ar-H), 7.46 (d, ^{3}J(H,H) = 8.7, 2H, Ar-H), 7.39 (d, ^{3}J(H,H) = 8.3, 2H, Ar-H), 6.96 (d, ^{3}J(H,H) = 8.7, 2H, Ar-H), 4.48 (m, 1H, OCH), 4.17 (dd, ^{2}J(H,H) = 8.4, ^{3}J(H,H) = 6.4, 1H, OCH_2), 4.08 (dd, ^{2}J(H,H) = 9.5, ^{3}J(H,H) = 5.4, 1H, OCH_2), 3.96 (dd, ^{2}J(H,H) = 9.5, ^{3}J(H,H) = 5.8, 1H, OCH_2), 3.90 (dd, ^{2}J(H,H) = 8.5, ^{3}J(H,H) = 5.8, 1H, OCH_2), 1.46 (s, 3H, CH_3), 1.40 (s, 3H, CH_3).

4'-[(2,2-Dimethyl-1,3-dioxolane-4-yl)methoxy]biphenyl-4-ylboronic acid (2)

1 (14.9 g, 0.041 mol) was dissolved in dry THF (250 mL) under an argon atmosphere. The solution was cooled to -85 °C and n-BuLi (27.7 ml of a 1.6 M Lösung in n-hexane, 0.044 mol) was added dropwise at this temperature. After stirring at this temperature for additional 15 min, trimethylborate (15 ml, 0.124 mol) was carefully added dropwise, so that the temperature does not exceed -85 °C. Stirring was continued and the mixture was allowed to warm to ambient temperature ovemight. Then phosphate-buffer (Sörensen, pH = 4.5 - 5.0; 81.6 ml KH_2PO_4-solution. + 0.8 ml Na_2HPO_4-solution) was added. After stirring for an additional hour, Et_2O (75 mL) was added and the layers were separated. The aqueous layer was extracted with Et_2O (4 x 50 mL). The combined organic layers were washed with water (3 x 20 mL) and brine (3 x 20 ml) and were dried with Na_2SO_4. After evaporation of the solvent the residue was suspended in hot $CHCl_3$. After cooling the precipitate was succed off. The crude product was used for the next step. Yield 12.8 g (0.039 mol, 95 %); colorless solid, mp.: 205-210 °C; ^{1}H-NMR (Aceton-D6, J/Hz, 400 MHz) δ = 7.92 (d, ^{3}J(H,H) = 8.3, 2H, Ar-H), 7.61 (d, ^{3}J(H,H) = 8.9, 2H, Ar-H), 7.59 (d, ^{3}J(H,H) = 8.3, 2H, Ar-H), 7.05 (d, ^{3}J(H,H) = 8.9, 2H, Ar-H), 4.46 (m, 1H, OCH), 4.16 (dd, ^{2}J(H,H) = 8.3, ^{3}J(H,H) = 6.4, 1H, OCH_2), 4.11-4.06 (m, 2H, OCH_2), 3.87 (dd, ^{2}J(H,H) = 8.3, ^{3}J(H,H) = 6.2, 1H, OCH_2), 1.39 (s, 3H, CH_3), 1.33 (s, 3H, CH_3).

3-Benzyloxy-4,4''-bis[(2,2-dimethyl-1,3-dioxolane-4-yl)methoxy]-p-terphenyl (4-Bzl)

A mixture of **3** (10 g , 0.025 mol), **2** (9.18 g, 0.027 mol) $Pd(PPh_3)_4$, 1.5 g (1.27 mmol), gylme (150 ml) and sat. aq. $NaHCO_3$ (100 ml) was stirred under an argon atmosphere at reflux for 5 h. After cooling to room temperature the solvent was removed and the residue was extracted with $CHCl_3$ (3 x 50 ml). The combined organic layers were washed with water and brine. After drying over anhydrous Na_2SO_4, the solvent was removed under reduced pressure, the residue was purified by column chromatigraphy (eluent: CH_2Cl_2 /Et_2O, 97:3, V/V) and crystallized from $CDCl_3$/n-hexane (1:1, v/v). Colorless solid; yield: 10.5 g (17.6 mmol, 69 %); mp 125-128 °C; ^{1}H-NMR (CDCl3, J/Hz, 400 MHz) δ = 7.58-7.52 (m, 6H, Ar-H), 7.45 (d, ^{3}J(H,H) = 7.1, 2H, Ar-H), 7.41-7.28 (m, 3H, Ar-H), 7.21-7.15 (m, 2H, Ar-H), 7.02-6.97 (m, 3H, Ar-H), 5.16 (s, 2H, OCH_2Ph), 4.49 (m, 2H, OCH), 4.19-3.90 (m, 8H, OCH_2), 1.47 (s, 3H, CH_3), 1.43 (s, 3H, CH_3), 1.40 (s, 3H, CH_3), 1.38 (s, 3H, CH_3).

4,4''-Bis[(2,2-dimethyl-1,3-dioxolane-4-yl)methoxy]-p-terphenyl-3-ol (4)

4-Bzl (10.5 g, 17.6 mmol) was dissolved in THF (150 ml). Under an argon atmosphere cyclohene (40 ml) and $Pd(OH)_2$/C (0.6 g; 10% Pd) were added. The reaction mixture as refluxed for 14 h; the catalyst was filtered off and washed with hot THF. The solvent was evaporated and the crude product was purified by crystallization from THF/$CHCl_3$. Colorless solid; yield: 8.8 g (17.3 mmol, 98 %); mp.: 204-207 °C; ^{1}H-NMR ($CDCl_3$, J/Hz, 400 MHz) δ

= 7.58 (s, 4H, Ar-H), 7.54 (d, ^{3}J(H,H) = 8.7, 2H, Ar-H), 7.22 (d, ^{4}J(H,H) = 2.3, 1H, Ar-H), 7.08 (dd, ^{3}J(H,H) = 8.3, ^{4}J(H,H) = 2.3, 1H, Ar-H), 6.99-6.95 (m, 3H, Ar-H), 6.20 (s, 1H, OH), 4.49 (m, 2H, OCH), 4.19-4.05 (m, 5H, OCH_2), 3.97 (dd, ^{2}J(H,H) = 9.5, ^{3}J(H,H) = 6.0, 1H, OCH_2), 3.93-3.89 (m, 2H, OCH_2), 1.49 (s, 3H, CH_3), 1.46 (s, 3H, CH_3), 1.41 (s, 3H, CH_3), 1.40 (s, 3H, CH_3).

3.3 4,4''-Bis[(2,2-dimethyl-1,3-dioxolane-4-yl)methoxy]-3-alkoxy-p-terphenyls (5/*n*)

General procedure. - A mixture of **4** (1 eq.), 1-bromo n-alkane (1.1 eq.), K_2CO_3 (2 eq.) and tetrabutylammonium iodide (5 mg) in anhydrous MeCN (50 ml for each mmol **4**) was stirred under reflux for 6-24 h. After complete consumption of **4** (DC) the mixture was cooled to room temperature, the reaction mixture was poured into ice-water (50 ml) and the aqueous layer was extracted with diethyl ether (2 x 50 mL). The combined organic layers were washed with water (50 ml) and brine (50 ml). After drying over anhydrous Na_2SO_4, filtration and evaporation of the solvent, the crude product was purified by chromatography or crystallization.

4,4''-Bis[(2,2-dimethyl-1,3-dioxolane-4-yl)methoxy]-3-pentyloxy-p-terphenyl 5/5

Purified by crystallization from $CHCl_3$ /n-hexane, yield 89 %; colorless solid; mp.: 99-101 °C; $C_{35}H_{44}O_7$, M=576.72 g/mol; ^{1}H-NMR ($CDCl_3$, J/Hz, 400 MHz) δ = 7.58 (s, 4H, Ar-H), 7.54 (d, ^{3}J(H,H) = 8.7, 2H, Ar-H), 7.14-7.11 (m, 2H, Ar-H), 6.98 (dd, ^{3}J(H,H) = 8.7, ^{4}J(H,H) = 1.5, 3H, Ar-H), 4.49 (m, 2H, OCH), 4.19-3.96 (m, 9H, OCH_2), 3.91 (dd, ^{2}J(H,H) = 8.5, ^{3}J(H,H) = 5.8, 1H, OCH_2), 1.83 (tt, ^{3}J(H,H) = 6.6, ^{3}J(H,H) = 6.1, 2H, OCH_2CH_2), 1.47 (s, 3H, CH_3), 1.46 (s, 3H, CH_3), 1.46 (m, 2H, $OCH_2CH_2CH_2$), 1.40 (s, 3H, CH_3), 1.40 (s, 3H, CH_3), 1.40 (m, 2H, $OCH_2CH_2CH_2CH_2$), 0.93 (t, ^{3}J(H,H) = 7.3, 3H, CH_3).

4,4''-Bis[(2,2-dimethyl-1,3-dioxolane-4-yl)methoxy]-3-heptyloxy-p-terphenyl 5/7

Purified by columnn chromatography (CH_2Cl_2/ Et_2O, 98:2, V/V); yield 87 %; colorless solid; mp.: 93-95 °C; $C_{37}H_{48}O_7$, M=604.77 g/mol; ^{1}H-NMR ($CDCl_3$, J/Hz, 400 MHz) δ = 7.58 (s, 4H, Ar-H), 7.54 (d, ^{3}J(H,H) = 8.9, 2H, Ar-H), 7.14-7.11 (m, 2H, Ar-H), 6.98 (d, ^{3}J(H,H) = 8.9, 3H, Ar-H), 4.49 (m, 2H, OCH), 4.46-3.96 (m, 9H, OCH_2), 3.91 (dd, ^{2}J(H,H) = 8.5, ^{3}J(H,H) = 5.8, 1H, OCH_2), 1.82 (tt, ^{3}J(H,H) = 7.1, ^{3}J(H,H) = 7.9, 2H, OCH_2CH_2), 1.47 (s, 3H, CH_3), 1.46 (s, 3H, CH_3), 1.46 (m, 2H, $OCH_2CH_2CH_2$), 1.40 (s, 3H, CH_3), 1.40 (s, 3H, CH_3), 1.38-1.28 (m, 6H, CH_2), 0.88 (t, ^{3}J(H,H) = 6.8, 3H, CH_3).

4,4''-Bis[(2,2-dimethyl-1,3-dioxolane-4-yl)methoxy]-3-octyloxy-p-terphenyl 5/8

Purified by columnn chromatography (CH_2Cl_2/ Et_2O, 98:2, V/V); yield 85 %; colorless solid; mp.: 84-86 °C; $C_{38}H_{50}O_7$, M=618.8 g/mol; ^{1}H-NMR ($CDCl_3$, J/Hz, 400 MHz) δ = 7.58 (s, 4H, Ar-H), 7.54 (d, ^{3}J(H,H) = 8.9, 2H, Ar-H), 7.14-7.11 (m, 2H, Ar-H), 6.98 (dd, ^{3}J(H,H) = 8.8, ^{4}J(H,H) = 1.5, 3H, Ar-H), 4.49 (m, 2H, OCH), 4.19-3.96 (m, 9H, OCH_2), 3.91 (dd, ^{2}J(H,H) = 8.5, ^{3}J(H,H) = 5.8, 1H, OCH_2), 1.82 (tt, ^{3}J(H,H) = 6.8, ^{3}J(H,H) = 7.9, 2H, OCH_2CH_2), 1.47 (s, 3H, CH_3), 1.46 (s, 3H, CH_3), 1.46 (m, 2H, $OCH_2CH_2CH_2$), 1.40 (s, 3H, CH_3), 1.39 (s, 3H, CH_3), 1.32-1.28 (m, 8H, CH_2), 0.87 (t, ^{3}J(H,H) = 6.8, 3H, CH_3).

4,4''-Bis[(2,2-dimethyl-1,3-dioxolane-4-yl)methoxy]-3-nonyloxy-p-terphenyl 5/9

Purified by columnn chromatography (CH_2Cl_2/ Et_2O, 97:3, V/V); yield 85 %; colorless solid; mp.: 88-90 °C; $C_{39}H_{52}O_7$, M=632.83 g/mol; ^{1}H-NMR ($CDCl_3$, J/Hz, 400 MHz) δ = 7.58 (s,

4H, Ar-H), 7.54 (d, ^{3}J(H,H) = 8.9, 2H, Ar-H), 7.13-7.11 (m, 2H, Ar-H), 6.98 (d, ^{3}J(H,H) = 8.7, 3H, Ar-H), 4.49 (m, 2H, OCH), 4.19-3.96 (m, 9H, OCH_2), 3.91 (dd, ^{2}J(H,H) = 8.3, ^{3}J(H,H) = 5.8, 1H, OCH_2), 1.82 (tt, ^{3}J(H,H) = 6.9, ^{3}J(H,H) = 7.9, 2H, OCH_2CH_2), 1.47 (s, 3H, CH_3), 1.46 (s, 3H, CH3), 1.46 (m, 2H, $OCH_2CH_2CH_2$), 1.40 (s, 3H, CH_3), 1.40 (s, 3H, CH_3), 1.35-1.28 (m, 10H, CH_2), 0.87 (t, ^{3}J(H,H) = 6.6, 3H, CH_3).

3-Decyloxy-4,4''-bis[(2,2-dimethyl-1,3-dioxolane-4-yl)methoxy]-p-terphenyl 5/10

Purified by columnn chromatography (CH_2Cl_2/ Et_2O, 98:2, V/V); yield 71 %; colorless solid; mp.: 92-95 °C; $C_{40}H_{54}O_7$, M=646.85 g/mol; ^{1}H-NMR ($CDCl_3$, J/Hz, 400 MHz) δ = 7.58 (s, 4H, Ar-H), 7.54 (d, ^{3}J(H,H) = 8.9, 2H, Ar-H), 7.13-7.11 (m, 2H, Ar-H), 6.98 (dd, ^{3}J(H,H) = 8.7, ^{4}J(H,H) = 1.5, 3H, Ar-H), 4.49 (m, 2H, OCH), 4.20-3.96 (m, 9H, OCH_2), 3.91 (dd, ^{2}J(H,H) = 8.5, ^{3}J(H,H) = 5.8, 1H, OCH_2), 1.82 (tt, ^{3}J(H,H) = 7.1, ^{3}J(H,H) = 7.9, 2H, OCH_2CH_2), 1.47 (s, 3H, CH_3), 1.46 (s, 3H, CH_3), 1.46 (m, 2H, $OCH_2CH_2CH_2$), 1.40 (s, 3H, CH_3), 1.40 (s, 3H, CH_3), 1.30-1.26 (m, 12H, CH_2), 0.87 (t, ^{3}J(H,H) = 6.6, 3H, CH_3).

4,4''-Bis[(2,2-dimethyl-1,3-dioxolane-4-yl)methoxy]-3-undecyloxy-p-terphenyl 5/11

Purified by columnn chromatography (CH_2Cl_2/ Et_2O, 97:3, V/V); yield 84 %; colorless solid; mp.: 93-95 °C; $C_{41}H_{56}O_7$, M=660.88 g/mol; ^{1}H-NMR ($CDCl_3$, J/Hz, 400 MHz) δ = 7.58 (s, 4H, Ar-H), 7.54 (d, ^{3}J(H,H) = 8.9, 2H, Ar-H), 7.13-7.11 (m, 2H, Ar-H), 6.98 (dd, ^{3}J(H,H) = 8.7, ^{4}J(H,H) = 1.5, 3H, Ar-H), 4.49 (m, 2H, OCH), 4.47-3.96 (m, 9H, OCH_2), 3.91 (dd, ^{2}J(H,H) = 8.5, ^{3}J(H,H) = 5.8, 1H, OCH_2), 1.82 (tt, ^{3}J(H,H) = 7.1, ^{3}J(H,H) = 7.7, 2H, OCH_2CH_2), 1.47 (s, 3H, CH_3), 1.46 (s, 3H, CH_3), 1.46 (m, 2H, $OCH_2CH_2CH_2$), 1.40 (s, 3H, CH_3), 1.40 (s, 3H, CH_3), 1.25 (bs, 14H, CH_2), 0.86 (t, ^{3}J(H,H) = 6.6, 3H, CH_3).

4,4''-Bis[(2,2-dimethyl-1,3-dioxolane-4-yl)methoxy]-3-dodecyloxy-p-terphenyl 5/12

Used without further purification for the next step; yield 78 %; colorless solid; mp.: 94-97 °C; $C_{42}H_{58}O_7$, M=674.91 g/mol; ^{1}H-NMR ($CDCl_3$, J/Hz, 400 MHz) δ = 7.58 (s, 4H, Ar-H), 7.54 (d, ^{3}J(H,H) = 8.7, 2H, Ar-H), 7.14-7.11 (m, 2H, Ar-H), 6.98 (dd, ^{3}J(H,H) = 8.7, ^{4}J(H,H) = 1.5, 3H, Ar-H), 4.49 (m, 2H, OCH), 4.20-3.96 (m, 9H, OCH_2), 3.91 (dd, ^{2}J(H,H) = 8.3, ^{3}J(H,H) = 5.8, 1H, OCH_2), 1.82 (tt, ^{3}J(H,H) = 7.1, ^{3}J(H,H) = 7.7, 2H, OCH_2CH_2), 1.47 (s, 3H, CH_3), 1.46 (s, 3H, CH_3), 1.46 (m, 2H, $OCH_2CH_2CH_2$), 1.40 (s, 3H, CH_3), 1.40 (s, 3H, CH_3), 1.35-1.25 (m, 16H, CH_2), 0.86 (t, ^{3}J(H,H) = 6.6, 3H, CH_3).

4,4''-Bis[(2,2-dimethyl-1,3-dioxolane-4-yl)methoxy]-3-tridecyloxy-p-terphenyl 5/13

Purified by columnn chromatography (CH_2Cl_2/ Et_2O, 98:2, V/V); yield 74 %; colorless solid; mp.: 92-95 °C; $C_{43}H_{60}O_7$, M=688.93 g/mol; ^{1}H-NMR ($CDCl_3$, J/Hz, 400 MHz) δ = 7.58 (s, 4H, Ar-H), 7.54 (d, ^{3}J(H,H) = 8.7, 2H, Ar-H), 7.24-7.12 (m, 2H, Ar-H), 6.98 (dd, ^{3}J(H,H) = 8.7, ^{4}J(H,H) = 1.3, 3H, Ar-H), 4.49 (m, 2H, OCH), 4.19-3.96 (m, 9H, OCH_2), 3.91 (dd, ^{2}J(H,H) = 8.5, ^{3}J(H,H) = 5.8, 1H, OCH_2), 1.82 (tt, ^{3}J(H,H) = 7.5, ^{3}J(H,H) = 7.3, 2H, OCH_2CH_2), 1.47 (s, 3H, CH_3), 1.46 (s, 3H, CH_3), 1.46 (m, 2H, $OCH_2CH_2CH_2$), 1.40 (s, 3H, CH_3), 1.40 (s, 3H, CH_3), 1.35-1.25 (m, 18H, CH_2), 0.86 (t, ^{3}J(H,H) = 6.7, 3H, CH_3).

4,4''-Bis[(2,2-dimethyl-1,3-dioxolane-4-yl)methoxy]-3-tetradecyloxy-p-terphenyl 5/14

Purified by columnn chromatography (CH_2Cl_2/ Et_2O, 98:2, V/V); yield 72 %; colorless solid; mp.: 88-90 °C; $C_{44}H_{62}O_7$, M=702.96 g/mol; ^{1}H-NMR ($CDCl_3$, J/Hz, 400 MHz) δ = 7.58 (s, 4H, Ar-H), 7.54 (d, ^{3}J(H,H) = 8.7, 2H, Ar-H), 7.13-7.11 (m, 2H, Ar-H), 6.98 (d, ^{3}J(H,H) =

8.7, 3H, Ar-H), 4.49 (m, 2H, OCH), 4.19-3.96 (m, 9H, OCH_2), 3.91 (dd, ^{2}J(H,H) = 8.5, ^{3}J(H,H) = 5.8, 1H, OCH_2), 1.82 (tt, ^{3}J(H,H) = 6.8, ^{3}J(H,H) = 7.9, 2H, OCH_2CH_2), 1.47 (s, 3H, CH_3), 1.46 (s, 3H, CH_3), 1.46 (m, 2H, $OCH_2CH_2CH_2$), 1.40 (s, 3H, CH_3), 1.39 (s, 3H, CH_3), 1.35-1.24 (m, 20H, CH_2), 0.86 (t, ^{3}J(H,H) = 6.4, 3H, CH_3).

3.4 4,4''-Bis(2,3-dihydroxypropyloxy)-3-alkoxy-p-terphenyls A/*n*

A mixture of **5/n** (~ 0.5 mmol) and PPTS (20 mg) in MeOH/THF (30 mL/20 ml) was heated to reflux for 6-24 h. The progress of the reaction was monitored by TLC. After cooling to 20 °C water (200 ml) was added and the mixture was extracted with $CHCl_3$ untill all precipitate is dissolved (~3 x 50 ml). The organic solutions were washed with water (50 ml), sat. $NaHCO_3$ (50 ml) and brine (50 mL). The solvent was evaporated and the crude product was purified by repeated crystallization.

4,4''-Bis(2,3-dihydroxypropyloxy)-3-pentyloxy-p-terphenyl A5

Purified by crystallization from MeOH/THF; yield 74 %; colorless solid; $C_{29}H_{36}O_7$, M=496.59 g/mol; ^{1}H-NMR (DMSO-D_6, J/Hz, 400 MHz) δ = 7.66-7.64 (m, 4H, Ar-H), 7.60 (d, ^{3}J(H,H) = 8.7, 2H, Ar-H), 7.22 (d, ^{4}J(H,H) = 2.1, 1H, Ar-H), 7.18 (dd, ^{3}J(H,H) = 8.3, ^{4}J(H,H) = 2.1, 1H, Ar-H),7.01 (t, ^{3}J(H,H) = 8.5, 3H, Ar-H), 4.91 (d, ^{3}J(H,H) = 5.0, 1H, OH), 4.83 (d, ^{3}J(H,H) = 5.2, 1H, OH), 4.62 (t, ^{3}J(H,H) = 5.6, 1H, OH), 4.56 (t, ^{3}J(H,H) = 5.6, 1H, OH), 4.05-3.95 (m, 4H, OCH, OCH_2), 3.90-3.86 (m, 2H, OCH_2),3.80-3.76 (m, 2H, OCH_2), 3.49-3.41 (m, 4H, OCH_2), 1.72 (tt, ^{3}J(H,H) = 6.8, ^{3}J(H,H) = 7.5, 2H, OCH_2CH_2), 1.44-1.31 (m, 4H, CH_2), 0.88(t, ^{3}J(H,H) = 7.3, 3H, CH_3). ^{13}C-NMR (DMSO-D_6, 100 MHz) δ = 158.2, 149.4,138.7, 138.6, 132.4, 128.0, 127.2, 126.9,119.4, 115.5, 115.1, 71.3, 70.6, 70.5, 70.3, 69.2, 63.5, 63.3, 29.2, 28.4, 22.5, 14.6. Analysis: calcd. for $C_{29}H_{36}O_7$*0.6 H_2O: C 68.64 %, H 7.39 %, found.: C 68.65 %, H 7.29 %.

4,4''-Bis(2,3-dihydroxypropyloxy)-3-heptyloxy-p-terphenyl A7

Purified by crystallization from MeOH/THF; yield 79 %; colorless solid;, M=524.65 g/mol; ^{1}H-NMR (DMSO-D_6, J/Hz, 400 MHz) δ = 7.67-7.64 (m, 4H, Ar-H), 7.60 (d, ^{3}J(H,H) = 8.7, 2H, Ar-H), 7.21 (d, ^{4}J(H,H) = 1.9, 1H, Ar-H), 7.18 (dd, ^{3}J(H,H) = 8.3, ^{4}J(H,H) = 2.1, 1H, Ar-H),7.01 (t, ^{3}J(H,H) = 8.1, 3H, Ar-H), 4.05-3.95(m, 4H, OCH, OCH_2), 3.90-3.86 (m, 2H, OCH_2), 3.81-3.76 (m, 2H, OCH_2), 3.49-3.40 (m, 4H, OCH_2), 1.71 (tt, ^{3}J(H,H) = 7.1, ^{3}J(H,H) = 7.7, 2H, OCH_2CH_2), 1.41 (m, 2H, $OCH_2CH_2CH_2$), 1.33-1.24 (m, 6H, CH_2),0.84 (t, ^{3}J(H,H) = 6.6, 3H, CH_3). ^{13}C-NMR (DMSO-D_6, 100 MHz) δ = 158.2, 148.7,148.2, 138.0, 137.9, 132.6, 131.7, 127.3, 126.5, 126.2,118.7, 114.8, 114.5, 112.3, 70.7, 69.9, 69.9, 69.6, 68.5, 62.8, 62.6, 31.2, 28.8, 28.4, 25.4, 22.0, 13.9. Analysis: calcd. for $C_{31}H_{40}O_7$: C 70.97 %, H 7.68 %, found: C 70.62 %, H 7.67 %.

4,4''-Bis(2,3-dihydroxypropyloxy)-3-octyloxy-p-terphenyl A8

Purified by crystallization from MeOH/THF; yield 80 %; colorless solid; $C_{32}H_{42}O_7$, M=538.67 g/mol; ^{1}H-NMR (DMSO-D_6, J/Hz, 400 MHz) δ = 7.67-7.64 (m, 4H, Ar-H), 7.60 (d, ^{3}J(H,H) = 8.7, 2H, Ar-H), 7.21 (d, ^{4}J(H,H) = 2.1, 1H, Ar-H), 7.18 (dd, ^{3}J(H,H) = 8.3, ^{4}J(H,H) = 2.1, 1H, Ar-H), 7.00 (t, ^{3}J(H,H) = 8.3, 3H, Ar-H), 4.91 (d, ^{3}J(H,H) = 5.2, 1H, OH), 4.83 (d, ^{3}J(H,H) = 5.2, 1H, OH), 4.63 (t, ^{3}J(H,H) = 5.6, 1H, OH), 4.56 (t, ^{3}J(H,H) = 5.6, 1H, OH), 4.05-3.95 (m, 4H, OCH, OCH_2), 3.90-3.86 (m, 2H, OCH_2), 3.80-3.75 (m, 2H, OCH_2), 3.47-3.41 (m, 4H, OCH_2), 1.70 (tt, ^{3}J(H,H) = 6.8, ^{3}J(H,H) = 7.7, 2H, OCH_2CH_2), 1.41 (m, 2H, $OCH_2CH_2CH_2$), 1.34-1.24 (m, 8H, CH_2), 0.83 (t, ^{3}J(H,H) = 6.4, ^{3}H, CH_3). ^{13}C-NMR (DMSO-

D_6, 100 MHz) δ = 158.2, 148.7,148.2, 138.0, 137.9, 132.6, 131.7, 127.3, 126.5, 126.2,118.7, 114.8, 114.4, 112.2, 70.6, 69.9, 69.8, 69.6, 68.5, 62.8, 62.6, 31.1, 28.8, 28.7, 28.6, 25.4, 22.0, 13.9. Analysis: calcd for $C_{32}H_{42}O_7$: C 71.35 %, H 7.86 %, found: C 71.10 %, H 7.80 %.

4,4''-Bis(2,3-dihydroxypropyloxy)-3-nonyloxy-p-terphenyl A9

Purified by crystallization from EtOH; yield 83 %; colorless solid; $C_{33}H_{44}O_7$, M=552.70 g/mol; ^{1}H-NMR (DMSO-D_6, J/Hz, 400 MHz) δ = 7.69-7.66 (m, 4H, Ar-H), 7.62 (d, ^{3}J(H,H) = 8.7, 2H, Ar-H), 7.24 (s, 1H,Ar-H), 7.21 (d, ^{3}J(H,H) = 8.3, 1H, Ar-H),7.04 (t, ^{3}J(H,H) = 8.1, 3H, Ar-H), 4.07-3.98(m, 4H, OCH, OCH_2), 3.93-3.88 (m, 2H,OCH_2), 3.82-3.78 (m, 2H, OCH_2), 3.49-3.45 (m, 4H, OCH_2), 1.73 (tt, ^{3}J(H,H) = 6.9, ^{3}J(H,H) = 7.5, 2H, OCH_2CH_2), 1.44 (m, 2H, $OCH_2CH_2CH_2$), 1.33-1.26 (m, 10H, CH_2), 0.85 (t, ^{3}J(H,H) = 6.4, 3H, CH_3). ^{13}C-NMR (DMSO-D_6, 100 MHz) δ = 158.2, 148.7,148.2, 138.0, 137.9, 132.6, 131.7, 127.3, 126.5, 126.2,118.7, 114.8, 114.5, 112.3, 70.6, 69.9, 69.8, 69.6, 68.5, 62.8, 62.6, 31.2, 28.9, 28.8, 28.7, 28.5, 25.4, 22.0, 13.9. Analysis: calcd. for $C_{33}H_{44}O_7$*0.15 H_2O: C 71.36 %, H 8.04 %, found: C 71.34 %, H 7.97 %.

3-Decyloxy-4,4''-bis(2,3-dihydroxypropyloxy)-p-terphenyl A10

Purified by crystallization from MeOH/THF; yield 89 %; colorless solid; $C_{34}H_{46}O_7$, M=566.72 g/mol; ^{1}H-NMR (DMSO-D_6, J/Hz, 400 MHz) δ = 7.67-7.63 (m, 4H, Ar-H), 7.60 (d, ^{3}J(H,H) = 8.9, 2H, Ar-H), 7.21 (d, ^{4}J(H,H) = 2.1, 1H, Ar-H), 7.18 (dd, ^{3}J(H,H) = 8.3, ^{4}J(H,H) = 2.1, 1H, Ar-H),7.01 (t, ^{3}J(H,H) = 8.1, 3H, Ar-H), 4.91 (d, ^{3}J(H,H) = 5.0, 1H, OH), 4.83 (d, ^{3}J(H,H) = 4.8, 1H, OH), 4.63 (t, ^{3}J(H,H) = 5.6, 1H, OH), 4.56 (t, ^{3}J(H,H) = 5.6, 1H, OH), 4.05-3.95 (m, 4H, OCH, OCH_2), 3.90-3.85 (m, 2H, OCH_2), 3.80-3.74 (m, 2H, OCH_2), 3.49-3.39 (m, 4H, OCH_2), 1.70 (tt, ^{3}J(H,H) = 7.1, ^{3}J(H,H) = 7.5, 2H, OCH_2CH_2), 1.41 (m, 2H, $OCH_2CH_2CH_2$), 1.34-1.20 (m, 12H, CH_2), 0.81 (t, ^{3}J(H,H) = 6.6, 3H, CH_3). ^{13}C-NMR (DMSO-D_6, 100 MHz) δ = 156.5, 147.1,146.6, 136.4, 136.3, 130.9, 130.1, 125.6, 124.8, 124.5,117.1, 113.2, 112.8, 110.7, 69.0, 68.3, 69.2, 68.0, 66.0, 61.1, 61.0, 29.5, 27.3, 27.2, 27.2, 27.0, 27.0, 23.8, 20.4, 12.2. Analysis: calcd. for $C_{34}H_{46}O_7$: C 72.06 %, H 8.18 %, found: C 71.77 %, H 8.10 %.

4,4''-Bis(2,3-dihydroxypropyloxy)-3-undecyloxy-p-terphenyl A11

Purified by crystallization from i-PropOH; yield 73 %; colorless solid; $C_{35}H_{48}O_7$, M=580.75 g/mol; ^{1}H-NMR (DMSO-D_6, J/Hz, 400 MHz) δ = 7.66-7.63 (m, 4H, Ar-H), 7.60 (d, ^{3}J(H,H) = 8.7, 2H, Ar-H), 7.21 (d, ^{4}J(H,H) = 1.9, 1H, Ar-H), 7.18 (dd, ^{3}J(H,H) = 8.3, ^{4}J(H,H) = 1.9, 1H, Ar-H),7.01 (t, ^{3}J(H,H) = 8.1, 3H, Ar-H), 4.21-3.95(m, 4H, OCH, OCH_2), 3.90-3.85 (m, 2H, OCH_2), 3.81-3.75 (m, 2H, OCH_2), 3.46-3.40(m, 4H, OCH_2), 1.70 (tt, ^{3}J(H,H) = 6.8, ^{3}J(H,H) = 7.5, 2H, OCH_2CH_2), 1.41 (m, 2H,$OCH_2CH_2CH_2$), 1.34-1.21 (m, 14H, CH_2),0.81 (t, ^{3}J(H,H) = 6.4, 3H, CH_3). ^{13}C-NMR (DMSO-D_6, 100 MHz) δ = 158.3, 148.8,148.3, 138.2, 138.0, 132.7, 131.8, 127.4, 126.6, 126.3,118.8, 114.9, 114.4, 112.3, 70.6, 69.9, 69.9, 69.7, 66.5, 62.8, 62.7, 31.2, 29.0, 28.8, 28.7, 28.6, 25.4, 22.0, 13.9. Analysis: cacd. for $C_{35}H_{48}O_7$: ber.: C 72.38 %, H 8.33 %, found: C 72.21 %, H 8.25 %.

4,4''-Bis(2,3-dihydroxypropyloxy)-3-dodecyloxy-p-terphenyl A12

Purified by crystallization from MeOH/THF; yield 81 %; colorless solid; $C_{36}H_{50}O_7$, M=594.78 g/mol; ^{1}H-NMR (DMSO-D_6, J/Hz, 400 MHz) δ = 7.64(d, ^{4}J(H,H) = 3.7, 4H, Ar-H), 7.59 (d, ^{3}J(H,H) = 8.9, 2H, Ar-H), 7.21 (d, ^{4}J(H,H) = 2.3, 1H, Ar-H), 7.18 (dd, ^{3}J(H,H) = 8.3, ^{4}J(H,H) = 2.3, 1H, Ar-H),7.01 (t, ^{3}J(H,H) = 8.1, 3H, Ar-H), 4.92 (d, ^{3}J(H,H) = 5.0, 1H,

OH), 4.83 (d, ^{3}J(H,H) = 5.2, 1H, OH), 4.63 (t, ^{3}J(H,H) = 5.4, 1H, OH), 4.56 (t, ^{3}J(H,H) = 5.8, 1H, OH), 4.05-3.95 (m, 4H, OCH, OCH_2), 3.90-3.85 (m, 2H, OCH_2),3.80-3.75 (m, 2H, OCH_2), 3.45-3.42 (m, 4H, OCH_2), 1.70 (tt, ^{3}J(H,H) = 6.8, ^{3}J(H,H) = 7.7, 2H, OCH_2CH_2), 1.41 (m, 2H, $OCH_2CH_2CH_2$), 1.37-1.20 (m, 16H, CH_2),0.81 (t, ^{3}J(H,H) = 6.6, 3H, CH_3). ^{13}C-NMR (DMSO-D_6, 100 MHz) δ = 158.9, 149.4,148.9, 138.7, 138.6, 133.3, 132.4, 128.0, 127.2, 126.9,119.4, 115.5, 115.2, 113.0, 71.4, 70.6, 70.6, 70.3, 69.2, 63.5, 63.3, 31.9, 29.7, 29.6, 29.6, 29.5, 29.4, 29.3, 26.1, 22.7, 14.6. Analysis: calcd. for $C_{36}H_{50}O_7$: C 72.70 %, H 8.47 %, found: C 72.51 %, H 8.42 %.

4,4''-Bis(2,3-dihydroxypropyloxy)-3-tridecyloxy-p-terphenyl A13

Purified by crystallization from MeOH/THF; yield 83 %; colorless solid; $C_{37}H_{52}O_7$, M=608.80 g/mol; ^{1}H-NMR (DMSO-D_6, J/Hz, 400 MHz) δ = 7.69-7.64 (m, 4H, Ar-H), 7.62 (d, ^{3}J(H,H) = 8.7, 2H, Ar-H), 7.24 (d, ^{4}J(H,H) = 2.1, 1H, Ar-H), 7.20 (dd, ^{3}J(H,H) = 8.3, ^{4}J(H,H) = 2.1, 1H, Ar-H),7.04 (t, ^{3}J(H,H) = 8.3, 3H, Ar-H), 4.07-3.98 (m, 4H, OCH, OCH_2), 3.93-3.88 (m, 2H, OCH_2), 3.82-3.78 (m, 2H, OCH_2), 3.51-3.45 (m, 4H, OCH_2), 1.73 (tt, ^{3}J(H,H) = 7.1, ^{3}J(H,H) = 7.7, 2H, OCH_2CH_2), 1.44 (m, 2H, $OCH_2CH_2CH_2$), 1.32-1.23 (m, 18H, CH_2), 0.84 (t, ^{3}J(H,H) = 6.4, 3H, CH_3). ^{13}C-NMR (DMSO-D_6, 100 MHz) δ = 158.2, 148.7,148.2, 138.0, 137.9, 132.6, 131.7, 127.3, 126.5, 126.2,118.7, 114.8, 114.4, 112.3, 70.6, 69.9, 69.8, 69.6, 68.5, 62.8, 62.6, 31.2, 28.9, 28.9, 28.9, 28.8, 28.7, 28.6, 25.4, 22.0, 13.8.
Analysis: cacld. for $C_{37}H_{52}O_7$: C 72.99 %, H 8.61 %, found: C 72.81 %, H 8.60 %.

4,4''-Bis(2,3-dihydroxypropyloxy)-3-tetradecyloxy-p-terphenyl A14

Purified by crystallization from MeOH/THF; yield 81 %; colorless solid; $C_{38}H_{54}O_7$, M=622.83 g/mol; ^{1}H-NMR (DMSO-D_6, J/Hz, 400 MHz) δ = 7.69-7.64 (m, 4H, Ar-H), 7.62 (d, ^{3}J(H,H) = 8.7, 2H, Ar-H), 7.24 (d, ^{4}J(H,H) = 2.1, 1H, Ar-H), 7.20 (dd, ^{3}J(H,H) = 8.3, ^{4}J(H,H) = 2.1, 1H, Ar-H),7.03 (t, ^{3}J(H,H) = 8.3, 3H, Ar-H), 4.94 (d, ^{3}J(H,H) = 5.2, 1H, OH), 4.86 (d, ^{3}J(H,H) = 5.2, 1H, OH), 4.66 (t, ^{3}J(H,H) = 5.8, 1H, OH), 4.58 (t, ^{3}J(H,H) = 5.6, 1H, OH), 4.07-3.98 (m, 4H, OCH, OCH_2), 3.93-3.88 (m, 2H, OCH_2), 3.82-3.79 (m, 2H, OCH_2), 3.50-3.44 (m, 4H, OCH_2), 1.72 (tt, ^{3}J(H,H) = 6.8, ^{3}J(H,H) = 7.5, 2H, OCH_2CH_2), 1.43-1.41 (m, 2H, $OCH_2CH_2CH_2$), 1.32-1.22 (m, 2H, CH_2),0.83 (t, ^{3}J(H,H) = 6.4, 3H, CH_3). ^{13}C-NMR (DMSO-D_6, 100 MHz) δ = 158.4, 148.9,148.4, 138.2, 138.1, 132.7, 131.9, 127.5, 126.7, 126.4,118.9, 115.0, 114.6, 112.5, 70.8, 70.1, 70.0, 69.8, 68.7, 63.0, 62.8, 31.4, 29.2, 29.1, 29.1, 29.0, 28.9, 28.8, 25.6, 22.2, 14.0. Analysis: calcd. for $C_{38}H_{54}O_7$: C 73.28 %, H 8.74 %, found: C 73.15 %, H 8.66 %.

4. References

S1 S. Lagerwall, A. Dahlgren,P. Jägemalm, P. Rudquist, K. D'have, H. Pauwels, R. Dabrowski, W. Drzewinski; *Adv. Funct. Mater*. 2001, 11, 87-94.

S2 A. Immirizi, B. Perini, *Acta Cryst.*, 1977, A33, 216-218.

S3 A. I. Kitaigorodski, *Molekülkristalle*, Akademieverlag: Berlin, Germany, 1979.

S4 V. VanRheenen, D. Y. Cha, W. M. Hartley, *Org. Synth.*, 1979, 58, 43.

S5 M. Kitamura, M. Isobe, Y. Ischikawa, T. Goto, *J. Am. Chem. Soc.* 1984, 106, 3252-3257.

S6 a) A. Suzuki, N. Miyaura, *J. Chem. Soc., Chem. Commun.*, 1979, 866-867; b) N. Miyaura, T. Yanagi, A. Suzuki, *Synth. Commun.*, 1981, 11, 513-519.

S7 K. Kindler, W. Peschke, *Justus Liebigs Ann. Chem.*, 1932, 497, 193-200.

S8 van Rijsbergen, R., Anteunis, M. J. O., De Bruyn, A. *J. Carbohydr. Chem*. 198, 32, 395-404.

S9 M. Kölbel, T. Beyersdorff, X. H. Cheng, C. Tschierske, J. Kain, S. Diele*, J. Am. Chem. Soc.* **2001**, *123*, 6809-6818.

S10 S. J. Richards, T. W. von Geldern, P. Jacobson, D. Wilcox, P. Nguyen, L. Öhman, M, Österlund, B. Gelius, M. Grynfarb, A. Goos-Nilsson, J. Wang, S. Fung, M. Kalmanovich, *Bioorg. Med. Chem. Lett*. **2006**, 16, 6086-6090. However, no data were given for this compound.